N78-10291

9733-1

CONS/~~733-1~~

NASA CR-135262

IMPROVED CERAMIC HEAT EXCHANGE MATERIAL

H. L. McCollister
OWENS-ILLINOIS, INC.
Toledo, Ohio

September 1977

Prepared for the
NATIONAL AERONAUTICS AND SPACE ADMINISTRATION
Lewis Research Center
Cleveland, Ohio 44135

Contract NAS 3-19733

As a part of the
ENERGY RESEARCH AND DEVELOPMENT ADMINISTRATION
Division of Transportation Energy Conservation
Heat Engine Highway Vehicle Systems Program

1. Report No.	2. Government Accession No.	3. Recipient's Catalog No.
NASA CR-135262		

4. Title and Subtitle	5. Report Date
Improved Ceramic Heat Exchange Material	September 1977
	6. Performing Organization Code

7. Author(s)	8. Performing Organization Report No.
H. L. McCollister	
	10. Work Unit No.

9. Performing Organization Name and Address	11. Contract or Grant No.
Owens-Illinois, Inc. P. O. Box 1035 Toledo, Ohio 43466	NAS 3-19733
	13. Type of Report and Period Covered
12. Sponsoring Agency Name and Address	Contractor Report
Energy Research and Development Administration Division of Transportation Energy Conservation Washington, D.C. 20545	14. Sponsoring Agency Code Report No. CONS/733-1

15. Supplementary Notes Interim Report. Prepared under Interagency Agreement EC-77-A-31-1011. Project Manager, Thomas P. Herbell, Materials and Structures Division, NASA Lewis Research Center, Cleveland, Ohio 44135

16. Abstract

The objective of this program is to develop improved corrosion resistant ceramic materials suitable for use as regenerative heat exchangers for vehicular gas turbines. Two glass-ceramic materials C-144 and C-145 have superior durability towards sulfuric acid and sodium sulfate compared to lithium aluminosilicate (LAS) Corning heat exchange material 9455. Material C-144 is a leached LAS material whose major crystalline phase is silica keatite plus mullite, and C-145 is a LAS keatite solid solution (S.S.) material. In comparison to material 9455, material C-144 is two orders of magnitude better in dimensional stability to sulfuric acid at 300°C, and one order of magnitude better in stability to sodium sulfate at 1000°C. Material C-145 is initially two times better in stability to sulfuric acid, and about one order of magnitude better in stability to sodium sulfate. Both C-144 and C-145 have less than 300 ppm $\Delta L/L$ thermal expansion from ambient to 1000°C, and good dimensional stability of less than $\sim$ 100 ppm $\Delta L/L$ after exposure to 1000°C for 100 hours. The glass-ceramic fabrication process produced a hexagonal honeycomb matrix having a 85% open frontal area, 50 μm wall thickness, and less than 5% porosity.

17. Key Words (Suggested by Author(s))	18. Distribution Statement
Ceramic Heat exchangers Corrosion resistant	Unclassified - unlimited STAR Category 27 ERDA Category UC-96

19. Security Classif. (of this report)	20. Security Classif. (of this page)	21. No. of Pages	22. Price*
Unclassified	Unclassified	34	A03

* For sale by the National Technical Information Service, Springfield, Virginia 22161

Summary

The objective of this program is to develop improved corrosion resistant ceramic materials suitable for use as regenerative heat exchangers for vehicular gas turbines. The major material requirements are low thermal expansion up to 1000°C, long time dimensional stability up to 1000°C, the ability to operate at least for short times up to 1100°C, and corrosion resistance.

In Task I, four crystalline glass-ceramic materials were studied in solid form as 2.5 cm O.D. x 3.8 cm rods. All materials 1, 2, C-144, and C-145 have improved resistance to chemical attack resulting from the presence of sulfuric acid and sodium salts which limits the life of Corning LAS 9455 heat exchange material.

Material 1 is composed of high quartz SS, material 2 contains keatite SS plus mullite, material C-144 is a leached LAS material whose major crystalline phase is silica keatite plus mullite, and material C-145 is composed of keatite SS.

Three of the candidate materials 2, C-144, and C-145, have strength, thermal expansion, thermal dimensional stability, and phase stability either better than or comparable to material 9455.

The most severe sulfuric acid attack on the candidate materials was more than an order of magnitude less than solid material 9454. Solid materials C-144 and C-145 showed no attack from sodium while materials 1 and 2 were marginally better than material 9454.

Materials C-144 and C-145 were chosen, based on their excellent resistance to sulfuric acid and sodium sulfate, to be fabricated into honeycomb matrix for property testing in Task II.

Results indicate that material C-144 is two orders of magnitude better than Corning LAS matrix 9455 in dimensional stability to sulfuric acid at 300°C. Material C-145 is twice as good as 9455 in dimensional stability to sulfuric acid after three exposure cycles and is about equal to 9455 after six cycles.

Sodium sulfate corrosion tests indicate that material C-144 is one order of magnitude better than material 9455 in stability to sodium sulfate at 1000°C after six exposure cycles. Material C-145 is one order of magnitude better than 9455 after three cycles and about four times better after six exposure cycles.

Both C-144 and C-145 have less than 300 ppm $\Delta L/L$ thermal expansion from ambient to 1000°C, and good dimensional stability of less than $\sim$ 100 ppm $\Delta L/L$ change in length after exposure to 1000°C for 100 hours. Materials 9455 and C-145 have better dimensional stability at 1100°C than material C-144 which contracts about 300 ppm $\Delta L/L$ after 10 hours while materials 9455 and C-145 expand less than 40 ppm $\Delta L/L$.

The glass-ceramic fabrication process of C-144 and C-145 produced a hexagonal isotropic honeycomb matrix having a passage diameter of 700 μm (0.028 in.), 50 μm (0.002 in.) wall thickness, 170 passages/cm^2 (1100/in.^{2}), 85% open frontal area, and less than 5% porosity. Because of the much thinner 50 μm wall, 450 KPa (65 psi) tensile strengths measured perpendicular to the open passages of C-144 and C-145 are low compared to the thicker walled (130-305 μm) 9455 anisotropic matrix which has a tensile strength of 1800 KPa (260 psi) in the radial direction and 4800 KPa (700 psi) in the tangential direction.

Table of Contents

Page

List of Tables

List of Figures

Figure

1. Introduction

The objective of this program is to develop ceramic materials suitable for use as regenerative heat exchangers for vehicular gas turbines. In Task I of contract NAS3-19733, four materials were investigated to overcome the chemical attack resulting from the presence of sulfuric acid and sodium which limit the life of lithium aluminosilicate (LAS) heat exchange materials. The four glass-ceramic candidate materials are:

1. A (LMAS) material whose major crystalline phase is high quartz solid solution (SS).

2. A (LAS) material whose major crystalline phase is keatite SS plus mullite.

3. CER-VIT$^{(R)}$ material C-144, a leached (LAS) material whose major crystalline phase is silica keatite plus mullite.

4. A (LAS) material whose major crystalline phase is keatite SS.

4-1 CER-VIT$^{(R)}$ material C-145, a silica compositional iteration to material 4 which produced an acceptable lower thermal expansion material.

The major material requirements are low thermal expansion up to 1000°C, long time dimensional stability up to 1000°C, and the ability to operate at least for short times up to 1100°C. The four candidate materials are designed to have strength, thermal expansion, thermal dimensional stability and phase stability, and thermal shock resistance comparable to the Corning 9454 solid material, but have improved corrosion resistance with respect to sulfuric acid and sodium salts. As a result of the materials testing program on bulk specimens carried out during Task I, all four candidate materials show superior corrosion resistance to both sulfuric acid at 300°C and sodium sulfate at 1000°C compared to material 9454. A summary of Task I test results is presented in Section 2.

Two of the candidate materials (3 and 4-1) were chosen, based on their excellent resistance to sulfuric acid and sodium sulfate, to be fabricated into honeycomb matrix for property testing under Task II. Material 3 has been designated Owens-Illinois CER-VIT$^{(R)}$ material C-144 and material 4-1 as CER-VIT$^{(R)}$ material C-145. As a result of the materials testing program on honeycomb specimens carried out in Task II, CER-VIT$^{(R)}$ materials C-144 and C-145 show superior corrosion resistance to both sulfuric acid and sodium sulfate compared to Corning matrix LAS 9455 heat exchange material. A summary of Task II test results is presented in Section 3.

2. Results and Discussion

Task I - Bulk Properties

As a result of the materials testing program on bulk specimens carried out during Task I of the contract, all four candidate materials show superior corrosion resistance to sulfuric acid at 300°C compared to Corning material 9454. Figure 1

$^{(R)}$CER-VIT is a registered trademark of Owens-Illnois, Inc.

shows that the most severe attack on the candidate materials is more than an order of magnitude less than material 9454. No reaction was observed for material C-144 after six exposure cycles as shown in Table 1.

Results of sodium sulfate corrosion tests as shown in Figure 2 indicate that no reaction was observed for material C-145 after six exposure cycles. The resistance of material C-144 to sodium sulfate is dependent on final thermal treatment as shown in Table 2. After three cycles, no reaction was observed for the C-144 material thermally treated at 1150°C.

Figures 3 through 8 show the expansion of material 9454 and candidate materials 1, 2, C-144 and C-145 after exposure to 1000°C for 1, 10, 28, 50, 75 and 100 hours, respectively. Three of the candidate materials (2, C-144 and C-145) have the desired thermal expansion from ambient to 1000°C of less than 800 ppm $\Delta L/L$ as shown in Figure 8 after thermal treatment at 1000°C for 100 hours.

Dimensional stability to 1000°C and 1100°C exposures has been determined as shown in Figures 9 and 10, respectively. None of the materials is as stable as material 9454; however, materials 2 and C-144 have acceptable dimensional stability. Material C-145 (Figure 9) contracts at 1000°C and starts to reach equilibrium after 1000°C for 75 hours, while thermal treatment at 1100°C (Figure 10) causes the material to expand. The effect of heat treatment temperature and resulting dimensional stability at 1000°C was investigated in Task II matrix testing and a C-145 material was produced which has good dimensional stability of less than $\sim$ 100 ppm $\Delta L/L$ change at 1000°C. Data of Young's modulus, Poisson's ratio and modulus of rupture are shown in Tables 3 and 4, respectively. Candidate materials 1, 2 and C-145 have higher Young's moduli and moduli of ruptures than material 9454. Data for material C-144 were not obtained because of the presence of microcracks in bulk specimens 1/2 cm thick which interfere with the sonic resonance test for determining Young's modulus. These microcracks are not present in thin-walled honeycomb matrix of material C-144.

Mercury porosimetry results indicate that materials 1, 2 and C-145 have a net pore volume of 0.002 cc/gram, while the chemically leached and thermally treated material C-144 has a net pore volume of 0.0098 cc/gram. The average pore diameter is 0.006 and 2.10 μm, respectively.

2.1 Sulfuric Acid

Specimens 2.5 cm diameter and 3.8 cm long were subjected to 900 milliliters of 96% sulfuric acid at 300°C for six exposure times. The specimens were contained in KIMAX(R) glass reaction vessels heated by Gas-col heating mantles. The acid is preheated in a separatory funnel and delivered hot to the reaction vessel which contained one specimen of each material. The acid temperature is controlled to $\pm$ 1°F by a thermocouple suspended into the acid.

Sulfuric acid reacts with LAS materials by exchanging hydrogen ions for lithium. This ion exchange reaction produces cracking in the microstructure if large specimen cross sections are involved. The depth of ion exchange is measured by optical microscopy. Figure 1 shows the reaction depth into the materials after 80 hours of 300°C sulfuric acid exposure.

Table 1 gives the reaction depth in millimeters vs. exposure time in sulfuric acid. The average reaction depth for three specimens is reported.

Further characterization of material C-144 indicates that the material has no weight loss after acid exposure. A change in specimen length of 13 ppm $\Delta L/L$ was measured after 80 hours of acid exposure at 300°C.

.2 Sodium Sulfate

In situ X-ray diffraction of sodium sulfate reacted specimen surfaces have been evaluated to determine the depth of ion exchange of Na for Li. Sodium expands the crystal lattice of LAS keatite and a marked change in crystal "D" spacing occurs in the ion exchanged surface layer. The depth of ion exchange on bulk specimens is obtained by mechanically grinding off the sodium sulfate exposed surface until no change in crystal "D" spacings is observed as compared to the original unreacted specimen surface.

The test consists of covering a specimen surface area of 3.4 cm with 0.0170 grams of anhydrous sodium sulfate and heating the coated specimen at 1000°C for 24 hours. Six exposure cycles are measured to determine the reaction depth. Material is ground off in 10 to μm intervals depending on the material and the extent of the surface reaction.

Figure 2 shows the reaction depth into the materials after six exposure cycles of sodium sulfate.

Table 2 shows the reaction depth for the materials after each 24 hour cycle. Corning material 9454 and material 2 (both LAS keatite materials) undergo an ion exchange of Na for Li when exposed to sodium sulfate as a marked change in crystal "D" spacing is observed by X-ray diffraction. Material 1, with a "stuffed" high quartz solid solution crystalline phase, does not show any change in crystal "D" spacings but the surface is altered by secondary crystallization forming (LAS) keatite S.S. and amorphous material with less intense high quartz S.S. crystalline peaks.

The resistance of material C-144 to sodium sulfate is dependent on final thermal treatment after acid leaching the lithia from the keatite structure as shown in Table 2. The reacted surface contains SiO_2 cristobalite; also, amorphous material is sometimes found.

Material C-145 looks very promising with respect to sodium sulfate resistance in that no reaction has been detected for the six exposures to sodium sulfate. Further testing of this material in sheets 0.7 to 1 mm in thickness with sodium sulfate applied to one surface indicates no warpage after 1000°C for 64 hours. Exposure cycles at 24 hour intervals indicate that warpage does occur after the third exposure. This is believed due to a build-up of fused salt on the materials surface which is measured after each application of sodium sulfate.

2.3 Thermal Expansion

The thermal expansion $\Delta L/L$ in ppm over the temperature range of ambient to 1000°C for the candidate materials and 9454 is shown in Figures 3 through 8. The standard deviation is 30 ppm $\Delta L/L$ for the three specimens measured. The thermal expansion specimens are cycled between ambient and 1000°C according to the following schedule:

1. ten cycles with a 1 hour hold at 1000°C

2. three cycles with a 6 hour hold at 1000°C

3. one cycle with a 22 hour hold at 1000°C

4. two cycles with a 25 hour hold at 1000°C

Thermal expansion was measured after exposure times at 1000°C for 1, 10, 28, 50, 75 and 100 hours. The specimen length was measured before and after each thermal exposure and thermal expansion test. Figure 9 shows the specimen length change ($\Delta L/L$ ppm) after thermal exposure to 1000°C.

2.4 Thermal Phase Stability

Thermal phase stability at 1100°C for all materials has been analyzed by X-ray diffraction. Corning material 9454 and materials 1, 2, C-144 and C-145 are stable for the 10 exposure cycles (ambient to 1100°C with a 1 hour hold for each cycle) with no change in crystal lattice parameter detected. Material 4 is not stable at 1100°C and contains larger amount of cristobalite in the range of 5-10 wt. % with increasing thermal exposure.

Dimensional stability at 1100°C is shown in Figure 10 for Corning material 9454 and the candidate materials. The average dimensional change $\Delta L/L$ ppm at 1100°C for three specimens is reported. Dimensional instability of material 4 can be attributed to the presence of cristobalite.

2.5 Elastic Modulus and Modulus of Rupture

No values were obtained for material C-144 because of the presence of some microcracks in the bulk specimens which interfere with the sonic resonance test. These microcracks are not present in thin-walled honeycomb matrix.

Values for Young's modulus and Poisson's ratios are shown in Table 3 for the other candidate materials.

Three specimens of each candidate material having dimensions of 11.4 x 1.9 x 1.3 cm were broken in four point flexure with the 11.4 x 1.9 cm surface being the tensile surface. The outer knife edge span was 8.9 cm and the inside span was 1.9 cm. Table 4 shows the modulus of rupture values obtained. All fractures started between the 1.9 cm span and were initiated in the plane of the specimen surface rather than at the edge.

3. Results and Discussion

Task II - Matrix Properties

Two of the candidate materials (C-144 and C-145) were chosen, based on their excellent resistance to sulfuric acid and sodium sulfate, to be fabricated into honeycomb matrix for property testing under Task II.

As a result of the materials testing program on honeycomb specimens carried out in Task II, CER-VIT$^{(R)}$ honeycomb C-144 and C-145 show superior corrosion resistance to sulfuric acid and sodium sulfate compared to Corning honeycomb 9455. Figure 11 shows that material C-144 is two orders of magnitude better than 9455 in dimensional

stability to sulfuric acid at 300°C. Material C-145 is twice as good as 9455 in dimensional stability to sulfuric acid after three exposure cycles and is about equal to 9455 after six cycles.

Results from sodium sulfate corrosion tests, as shown in Figure 13 and tabulated in Table 5, indicate that material C-144 is one order of magnitude better in stability to sodium sulfate at 1000°C after six exposure cycles than material 9455. Material C-145 is one order of magnitude better than 9455 after three cycles and about four times better after six exposure cycles.

Figures 14 through 19 show the expansion of materials 9455, C-144, C-144-1 and C-145 after exposure to 1000°C for 1, 10, 28, 50, 75 and 1000 hours, respectively. Both materials C-144 and C-145 have less than 600 ppm $\Delta L/L$ thermal expansion from ambient to 1000°C for the indicated times. Depending on thermal treatment, material C-144 can have either a negative expansion of -550 $\Delta L/L$ from ambient to 1000°C or a near-zero expansion (C-144-1) as indicated in Figures 14 through 19. However, C-144 as a negative expansion material has better dimensional stability to both sulfuric acid and sodium sulfate. Testing in this area will continue in Task V by comparing the corrosion resistance of C-144 with the Corning 9460 AS heat exchange material.

Dimensional stability of the candidate materials to 1000°C and 1100°C is shown in Figures 20 and 21, respectively. Materials 9455, C-144, C-144-1 and C-145 all have good dimensional stability of less than $\sim$ 100 ppm $\Delta L/L$ at 1000°C for the indicated times, while materials 9455 and C-145 have better dimensional stability at 1100°C than material C-144 which contracts about 300 ppm $\Delta L/L$ after 10 hours while materials 9455 and C-145 expand less than 40 ppm $\Delta L/L$.

Elastic modulus, modulus of rupture, and mercury porosimetry results are shown in Tables 6 and 7, respectively. Thin wall C-144 and C-145 matrixes have tensile strengths of $\sim$65 psi with less than 5% wall porosity.

3.1 Sulfuric Acid

Honeycomb specimens were immersed in 1% sulfuric acid, evacuated to remove air from the passages, and removed from the acid after 2 hours. Excess acid was allowed to drain from the honeycomb by gravity before inserting then into a furnace at 300°C for 2 hours to complete one cycle. Figure 11 shows the dimensional changes $\Delta L/L$ ppm after six exposure cycles.

Figure 12 shows the effect of a smaller acid concentration in that excess acid was allowed to drain from the honeycomb by gravity and then the matrix was shook twice which removed more acid. Material C-145 contracts with the weaker acid concentration, but expands by cracking with the more concentrated acid as a result of the H^+ for Li^+ ion exchange.

3.2 Sodium Sulfate

Minus 200 mesh reagent grade anhydrous sodium sulfate was dusted through the honeycomb matrix passages of materials 9455 and C-145 as evenly as possible until a specimen weight gain of 1/4% was measured. The specimens were exposed to 1000°C for 24 hours to complete one cycle. Results for six cycles are shown in Figure 13 and tabulated in Table 5. Material C-144 is two orders of magnitude better

in dimensional stability to sodium sulfate than 9455 after six cycles while material C-145 is an order of magnitude better than 9455 after three cycles and about four times better after six exposure cycles.

Comparison of Ford data and Owens-Illinois data vs. specimen cross sectional area as shown in Table 5 indicates a large amount of variability in dimensional change with exposure cycle. Dusting the matrix does not give a uniform distribution of sodium sulfate down the tube interior with majority of the sodium sulfate remaining near the specimens' ends producing large dimensional changes in honeycomb 9455.

3.3 Thermal Expansion

The thermal expansion $\Delta L/L$ in ppm over the temperature range of ambient to 1000°C for materials C-144, C-144-1, C-145, and 9455 is shown in Figures 14 through 19 after exposure to 1000°C for 1, 10, 28, 50, 75 and 100 hours, respectively. The standard deviation is 50 ppm $\Delta L/L$ for the three specimens measured.

The thermal expansion specimens were cycled between ambient and 1000°C according to the following schedule:

1. ten cycles with a 1 hour hold at 1000°C
2. three cycles with a 6 hour hold at 1000°C
3. one cycle with a 22 hour hold at 1000°C
4. two cycles with a 25 hour hold at 1000°C

Thermal expansion was measured after exposure times at 1000°C for 1, 10, 28, 50, 75 and 100 hours. The specimen length is measured before and after each thermal exposure. Figure 20 shows the specimen length change ($\Delta L/L$ ppm) after thermal exposure.

3.4 Thermal Phase Stability

Thermal phase stability at 1100°C for 9455, C-144 and C-145 has been analyzed by X-ray diffraction. Corning honeycomb 9455, C-144 and C-145 are stable for the 10 exposure cycles, ambient to 1100°C with a one hour hold for each cycle. Dimensional stability at 1100°C is shown in Figure 21 for materials 9455, C-144 and C-145.

3.5 Elastic Modulus and Modulus of Rupture

Modulus of rupture values shown in Table 6 were obtained using four-point flexure. The outer knife edge span was 8.9 cms and the inner span was 1.9 cm. Specimen dimensions were 11.4 x 1.9 x 1.3 cms with the 11.4 x 1.9 cm surface as the tensile surface. Stress rates were 700KPa per min. for tangential 9455 matrix and 200 KPa per min. for radial 9455 matrix and isotropic matrixes C-144 and C-145. Matrixes C-144 and C-145 have a high open frontal area of 85% compared to 9455 matrix which has 65% open frontal area. The lower strength values of approximately 450 KPa for C-144 and C-145 compared to 9455 matrix strengths of

1790 KPa (radial) and 4830 KPa (tangential) is attributed to the thinner 50 μm matrix wall thickness of C-144 and C-145 compared to the 130 to 305 μm wall of matrix 9455.

Elastic modulus values shown in Table 6 were obtained using the sonic resonance technique according to ASTM Standard C623-69T. These are tentative values since we have obtained the same published value for 9455 tangential specimens but are one order in magnitude higher for 9455 radial specimens. This discrepancy is due to matrix wall and void configuration which effect the ability to determine the resonance frequency. Strain gages will be used in future testing to determine the elastic modulus.

3.6 Microstructure and Porosity

Electron micrographs of solid materials 1 and 2 and matrix materials C-144 and C-145 are shown in Figure 22. Materials 2, C-144 and C-145 all have grain sizes less than 1 μm. Material 1 has a 2-1/2 μm grain size.

Mercury porosimetry results for matrix materials C-144, C-145, and 9455 are shown in Table 7.

Matrix C-145 has a calculated wall porosity of 5%; however, matrix C-145 has a near hexagonal cross section but at tube interstices a 50 μm dia. open area exists where the two glass tube walls did not bloat together. This open area may account for the 52 μ average dia. pore reported from mercury porosimetry. Because this open interstitial area influences the displacement density, a higher wall porosity is calculated than what is actually present. Matrix C-144 has a bimodal distribution of voids, 20 μm average dia. voids which may be because of the interstitial area between tubes and 0.01 μm average dia. voids in the tube walls as a result of leaching lithium from the material. The wall porosity will be investigated further for matrixes C-144 and C-145 after stuffing material has been added to the glass tube bloating process or other techniques are used to eliminate the open interstitial area. The interstitial area is not desirable from a seal bar wear standpoint because a single wall rather than a double wall thickness is present.

4. Conclusions

This investigation evaluated four glass-ceramic materials suitable for use as gas turbine heat exchangers. The purpose of the program was to develop improved corrosion resistant materials less susceptible to attack by sulfuric acid and sodium salts. Comparative tests of the new improved materials fabricated as solid and honeycomb matrix were made with 1st generation lithium aluminosilicate (LAS) Corning solid 9454 and heat exchanger matrix 9455.

Two of the glass-ceramic materials, C-144 and C-145, have superior durability towards sulfuric acid and sodium sulfate compared to Corning materials 9454 and 9455. Material C-144 is a leached LAS material whose major crystalline phase is silica keatite plus mullite. Material C-145 is composed of LAS keatite solid solution.

1. Material C-144 is two orders of magnitude better in dimensional stability to sulfuric acid at 300°C, and one order of magnitude better in stability to sodium sulfate at 1000°C compared to material 9455.

2. Material C-145 is initially two times better in stability to sulfuric acid at 300°C and about one order of magnitude better in stability to sodium sulfate at 1000°C compared to material 9455.

3. Materials C-144 and C-145 are either better than or comparable to material 9455 in physical properties. Materials C-144 and C-145 have less than 300 ppm $\Delta L/L$ thermal expansion from ambient to 1000°C, good dimensional stability of less than $\sim$ 100 ppm $\Delta L/L$ change in length after exposure to 1000°C for 100 hours and acceptable dimensional stability to short exposure times at 1100°C. Material C-145 expands less than 40 ppm $\Delta L/L$ after 1100°C for 10 hours while material C-144 contracts about 300 ppm $\Delta L/L$. Material 9455 has a 500 ppm $\Delta L/L$ thermal expansion from ambient to 1000°C, good dimensional stability of less than $\sim$ 100 ppm change in length after 1000°C for 100 hours, and has adequate dimensional stability at 1100°C expanding less than 40 ppm $\Delta L/L$ change in length after 10 hours.

4. The glass-ceramic fabrication process of C-144 and C-145 produced a hexagonal honeycomb matrix with a very thin wall thickness of 50 μm, a very high open frontal area of 85%, and a wall porosity of less than 5%. Because of the thin walls and high open frontal area, matrix honeycomb C-144 and C-145 have a lower tensile strength perpendicular to the open passages than material 9455. Honeycomb C-144 and C-145 have isotropic structures with tensile strengths of 450 KPa compared to the anisotropic structure of 9455 matrix which has a tensile strength of 1800 KPa in the radial direction and 4800 KPa in the tangential direction. The wall thickness of the 9455 matrix varies between 130 to 305 μm.

Table 1 - Depth of Sulfuric Acid Reaction (in millimeters)

H_2SO_4 at 300°C for	9454	1	2	C-144	4	C-145
6 hours	0.995	0.147	0.035	none detected	0.227	0.083
16 hours	2.13	0.233	0.089	"	0.306	0.164
32 hours	3.38	0.270	0.161	"	0.390	0.215
48 hours	4.77	0.292	0.198	"	0.443	0.224
64 hours	5.27	0.323	0.205	"	0.482	0.265
80 hours	6.40	0.420	0.237	"	0.544	0.310

Table 2 - Depth of Sodium Sulfate Reaction (μm)

Na_2SO_4 at 1000°C for 24 hours	9454	1	2	C-144 Heat Treatment Temperature (°C) 1150 - 1 hr	1200 - 1 hr			1200 - 16 hrs		C-145
% Cristobalite*				0	0	5	10	5	10	
1 Cycle	45	20	5	0	0	---	---	10	---	N**
2 Cycles	100	90	30	0		150	---		400	N
3 Cycles	155	100	45	0		550	200		900	N
4 Cycles	200	100	65				750			N
5 Cycles	205	135	90				1000			N
6 Cycles	230	205	130				***			N

* % of cristobalite detected as a function of depth measured from the specimen surface

** N - No reaction detected by X-ray diffraction

*** Sixth cycle was not completed because bulk specimens greater than ∿ 1 mm were not obtained because of cracking in leaching lithia from the LAS material

Table 3 - Young's Modulus

	Young's Modulus KPa x 10^{-6}	(Psi x 10^{-6})	Poisson's Ratio
Material 1	91.57	(13.28)	0.23
Material 2	76.12	(11.04)	0.25
Material C-144	--		--
Material 4	77.43	(11.23)	0.23
Material C-145	80.95	(11.74)	0.26
Material 9454	73.64	(10.68)	0.28

Table 4 - Modulus of Rupture

Material	Modulus of Rupture Strength KPa	(Psi)	Std. Deviation KPa	(Psi)	Time to Failure (sec.)	Load kgs.	(lbs.)
9454	69,600	(10,100)	5,500	(800)	27	204	(450)
1	93,800	(13,600)	5,500	(800)	31	259	(570)
2	90,300	(13,100)	6,900	(1000)	27	247	(545)
C-144	--	--	--	--	--	--	--
4	38,600	(5,600)	11,700	(1700)	16	120	(265)
C-145	104,100	(15,100)	8,300	(1200)	31	308	(680)

Table 5 - Dimensional Stability $\Delta L/L$ ppm to Sodium Sulfate at 1000°C for 24 Hr. Cycles Vs. Specimen Cross Sectional Area

Specimen	9455	9455	9455	C-144	C-145
Length cm		6.9	6.9	6.9	6.9
Cross Sectional Area cm^2	Ford Data*	1.6	4.5	4.8	4.8
Cycle					
1	175	2070	250	-95	30
2	400	2930	1800	-170	180
3	700	--	2200	-135	390
4	1250	--	2550	-170	490
5	1575	--	2830	-195	625
6	--	--	2990	-200	750

*COO-2630-15, Ford Progress Report, April 1976, "Automotive Gas Turbine Ceramic Regenerator Design and Reliability Program."

Table 6 - Modulus of Rupture and Elastic Modulus

	S		Young's Modulus x 10^{-6}		Matrix Wall Thickness		Open Frontal Area
	KPa	(Psi)	Kpa	(Psi)	µm	(mils)	%
9455							
Solid	68,950	(10,000)	73.64	(10.68)			
Matrix Radial	1,800	(260)	7.6	(1.1)			
Matrix Tangential	4,800	(700)	13.8	(2.0)	127-305	(5-12)	65
C-144							
Solid	--	--	--	--			
Matrix	410	(60)	1.0	(0.15)	50	(2)	85
C-145							
Solid	104,100	(15,100)	80.94	(11.74)			
Matrix	480	(70)	1.2	(0.18)	50	(2)	85

Table 7 - Matrix Porosity

Matrix	Net Pore Vol. (cc/g)	Aveg. Pore Dia. (μm)	Density (gm/cc)		
			Bulk	Displacement	Skeletal
9455	0.03362	7.4	.74	2.08*	2.28*
C-144	0.02898	0.01	.40	--	--
C-145	0.02188	52	.37	2.52	2.39

*Corning values

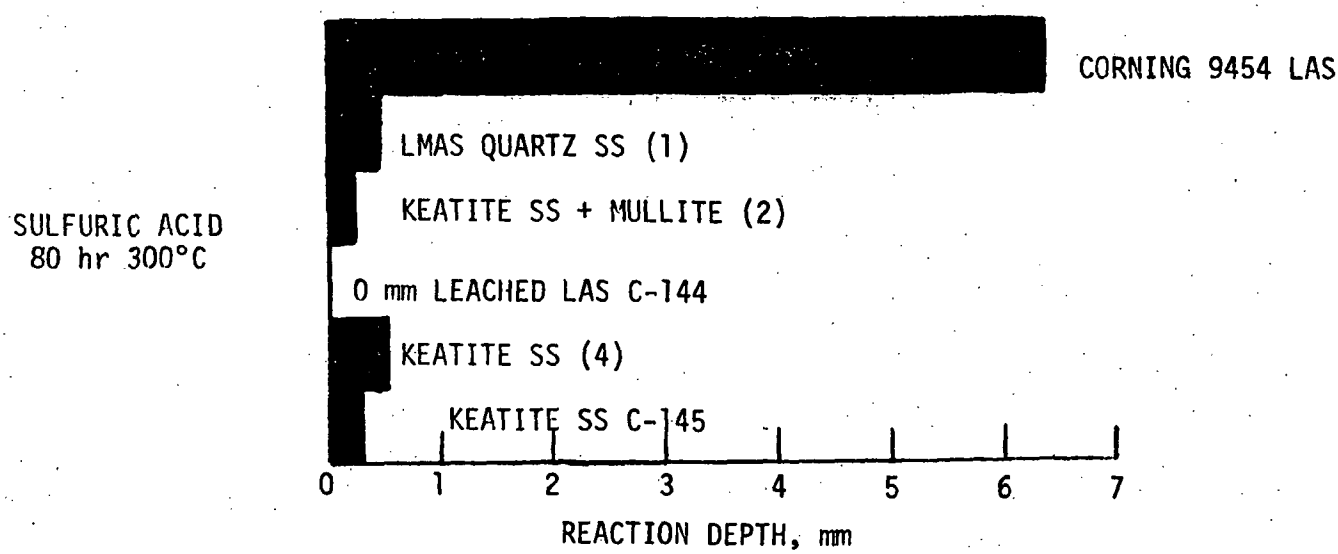

Figure 1 - Reaction Depth after 80 Hrs. of 300°C Sulfuric Acid

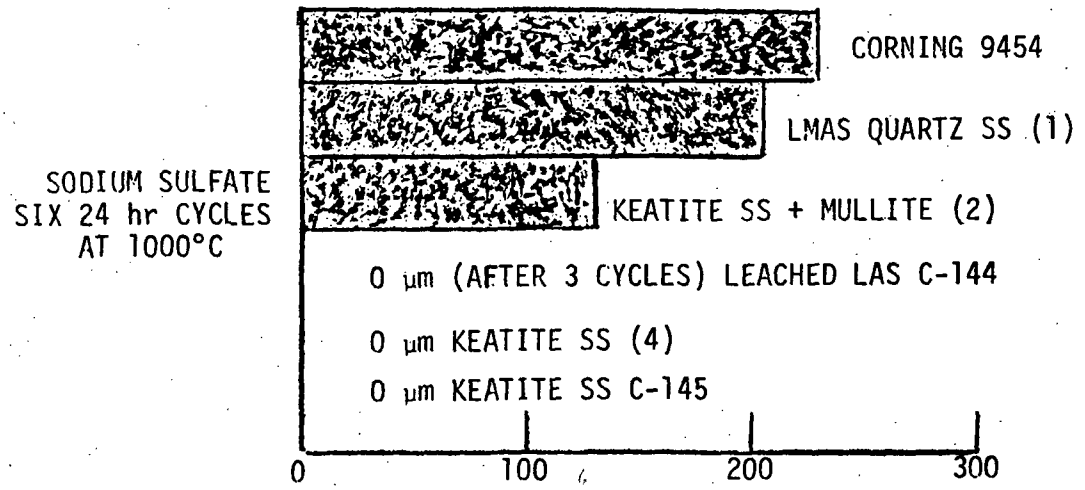

Figure 2 - Reaction Depth After Six 24 Hr Cycles of Sodium Sulfate at 1000°C

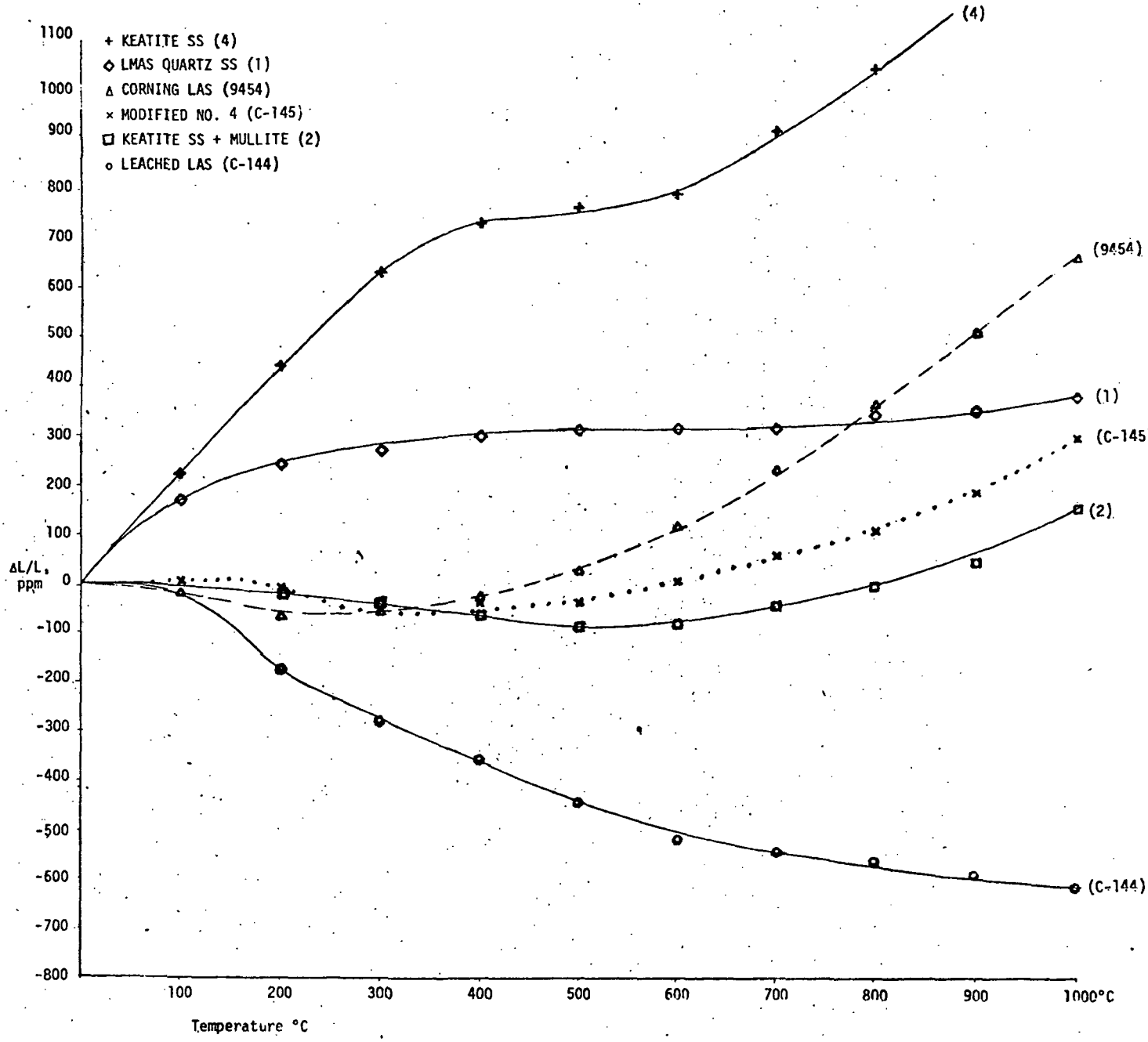

Figure 3 - Thermal Expansion of 9454 and Materials 1, 2, 3, 4 After 1000°C-1 Hr

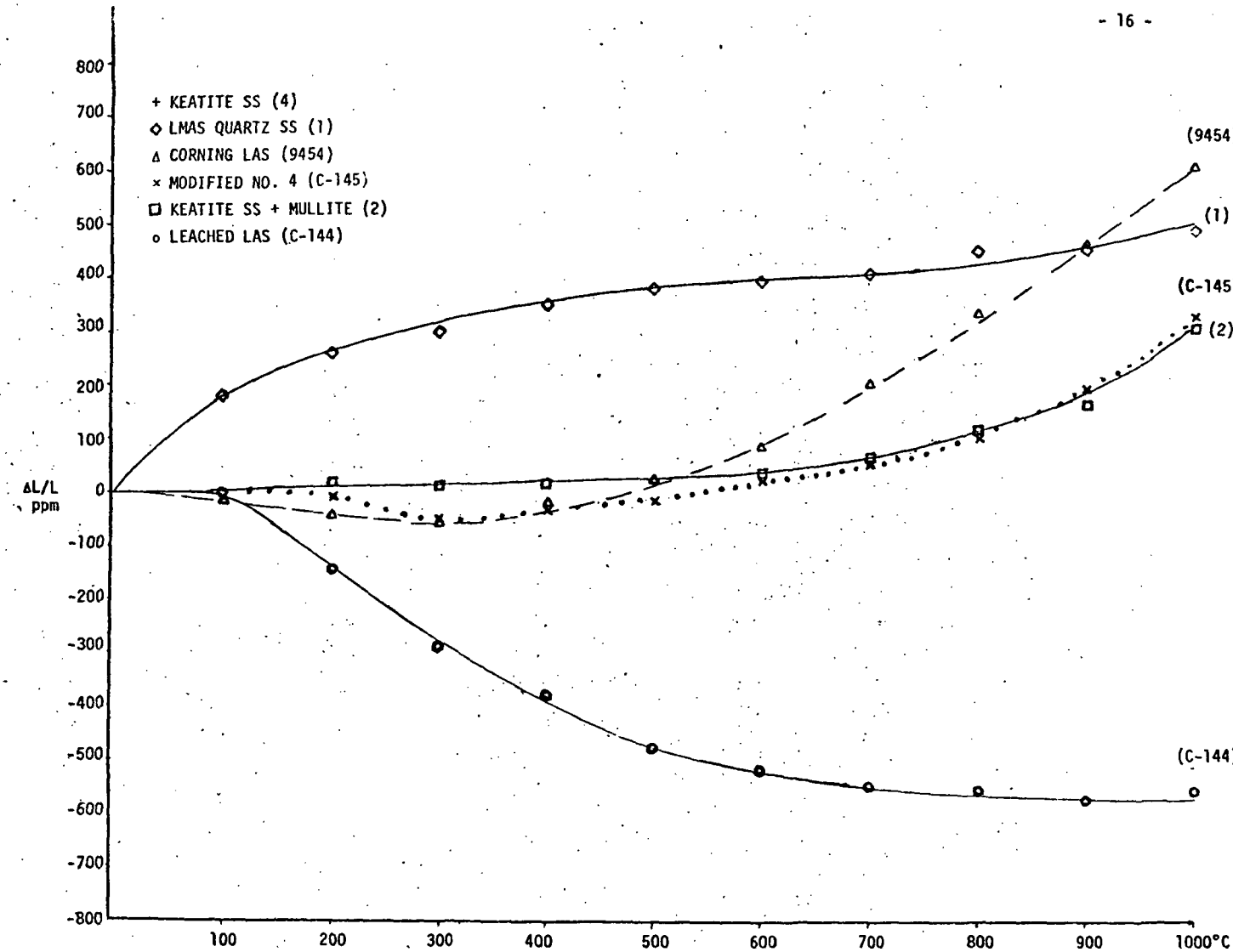

Figure 4 - Thermal Expansion of 9454 and Materials 1, 2, 3 After 1000°C-10 Hrs

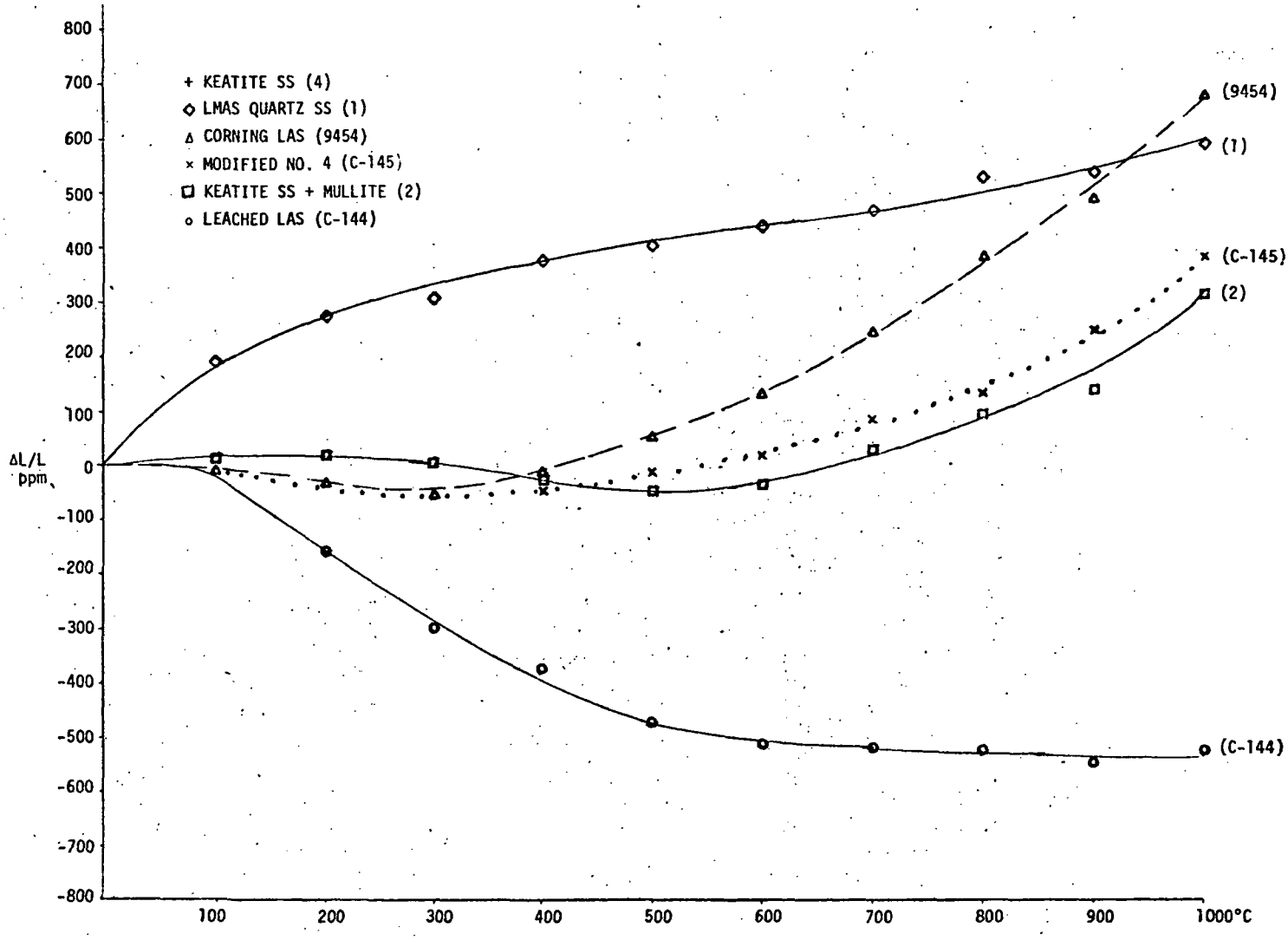

Figure 5 - Thermal Expansion of 9454 and Materials 1, 2, 3 After 1000°C-28 Hrs.

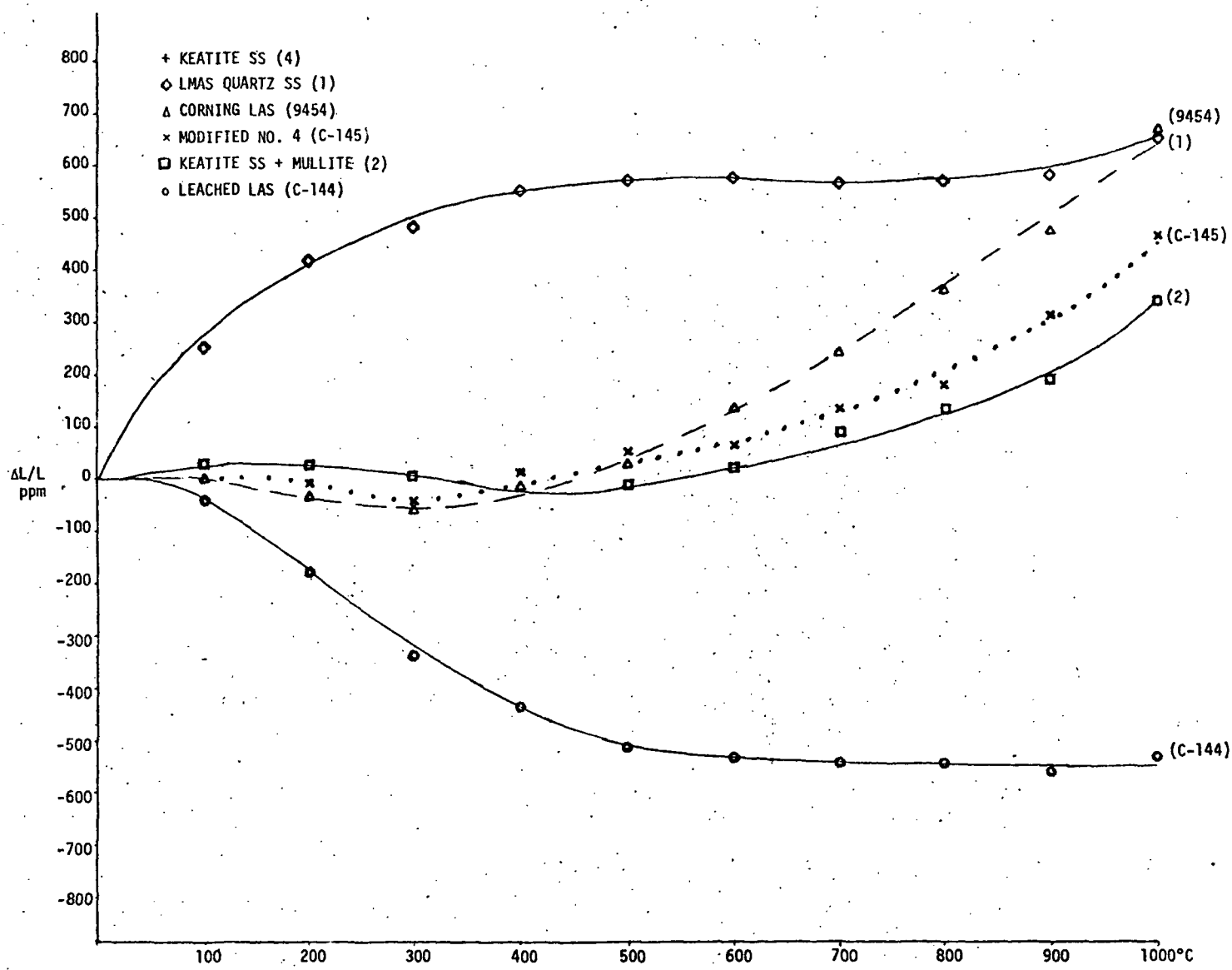

Figure 6 - Thermal Expansion of 9454 and Materials 1, 2, 3 After 1000°C-50 Hrs.

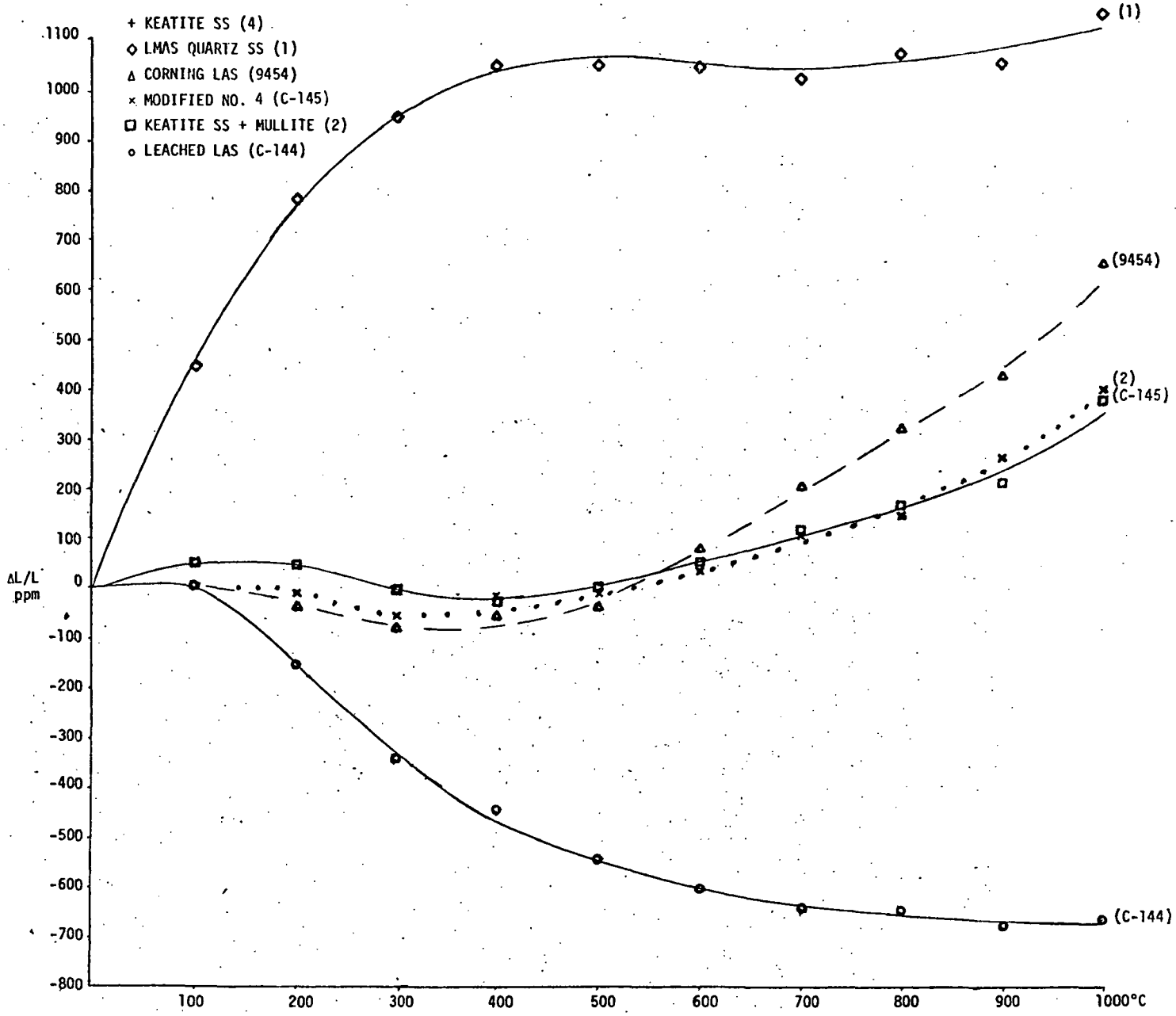

Figure 7 - Thermal Expansion of 9454 and Materials 1, 2, 3 After 1000°C-75 Hrs

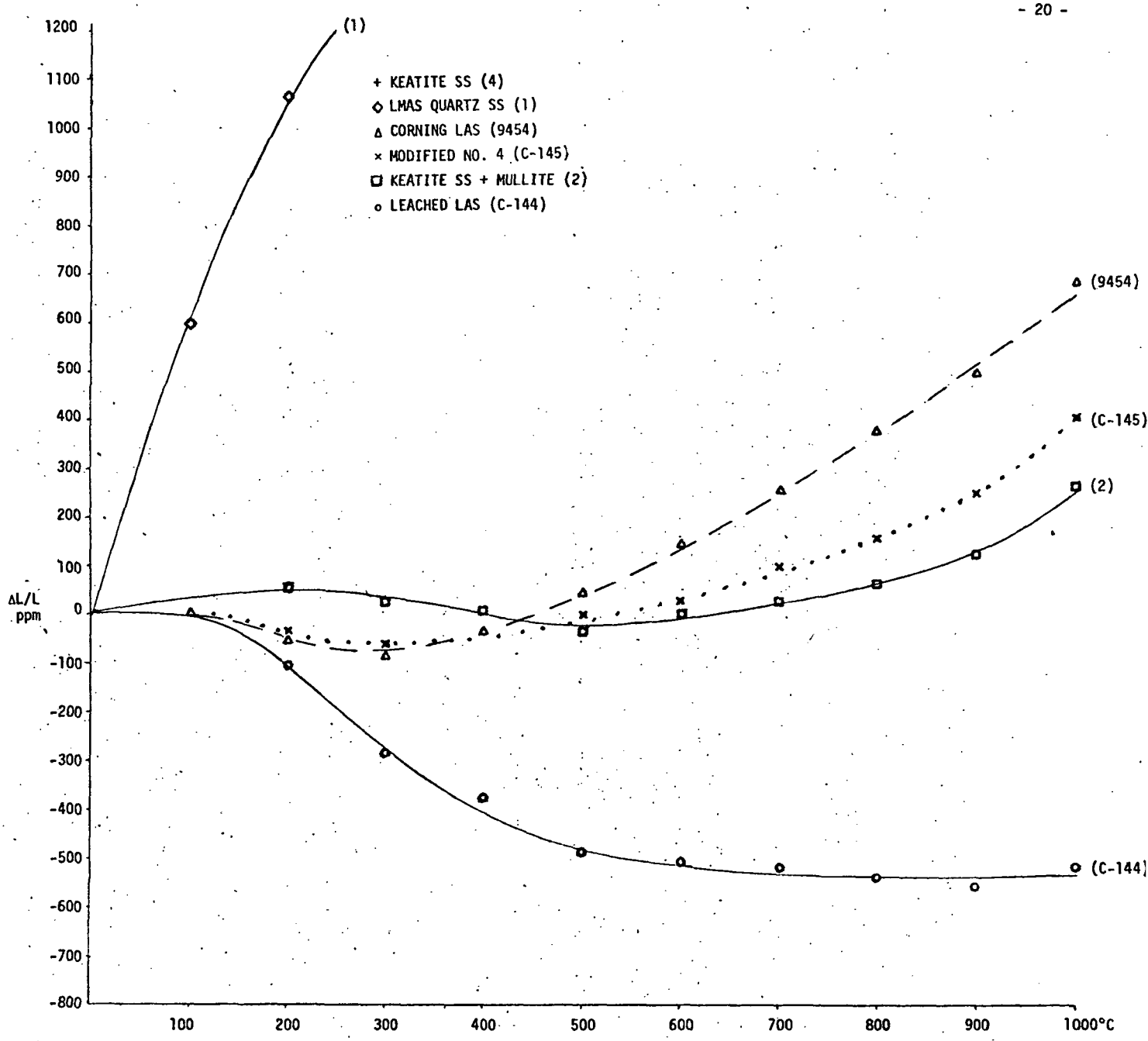

Figure 8 - Thermal Expansion of 9454 and Materials 1, 2, 3 After 1000°C-1000 Hrs

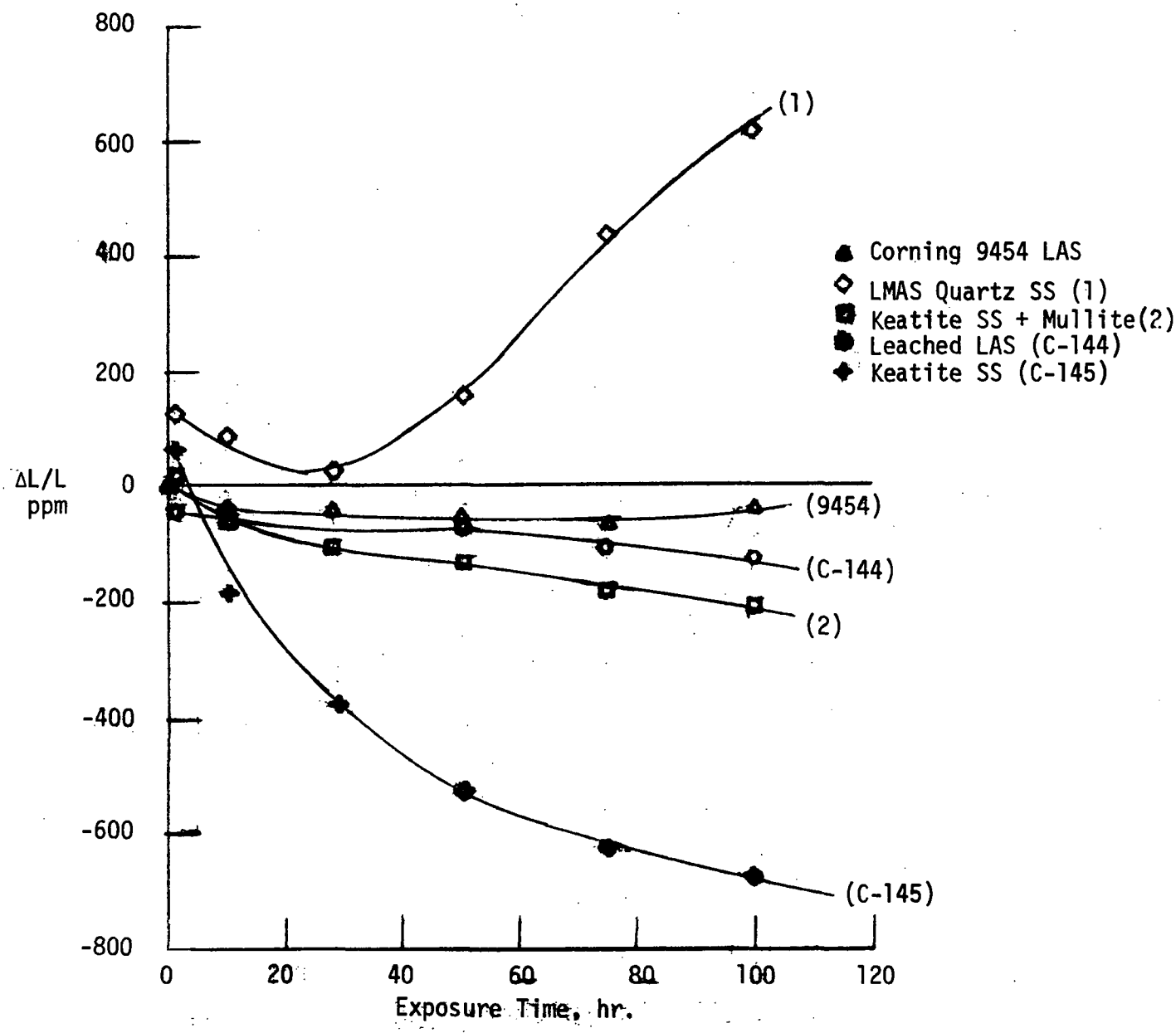

Figure 9 Dimensional Stability at 1000°C, Length Change after Exposure

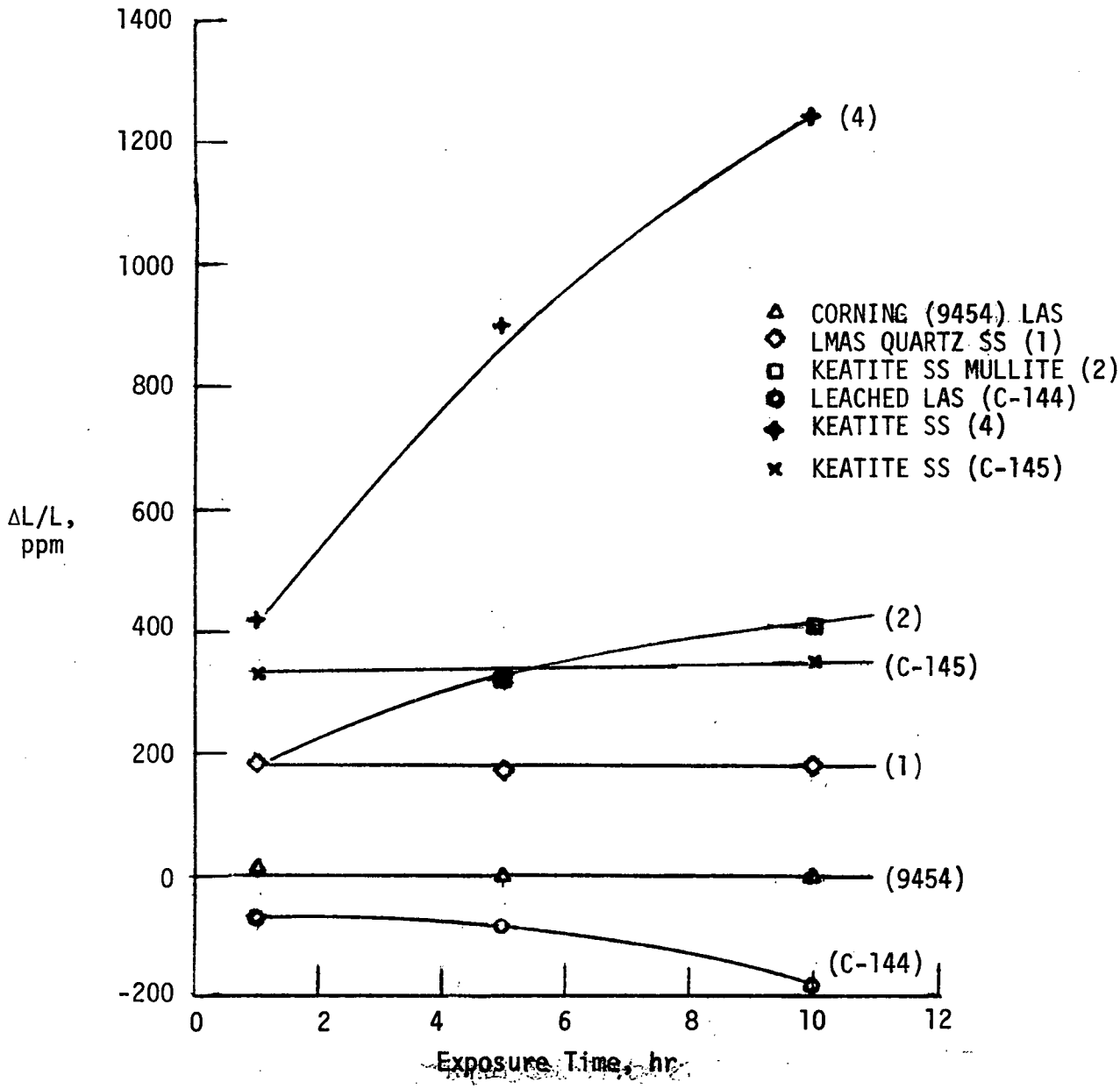

Figure 10 - Dimensional Stability at 1100°C, Length Change After Exposure

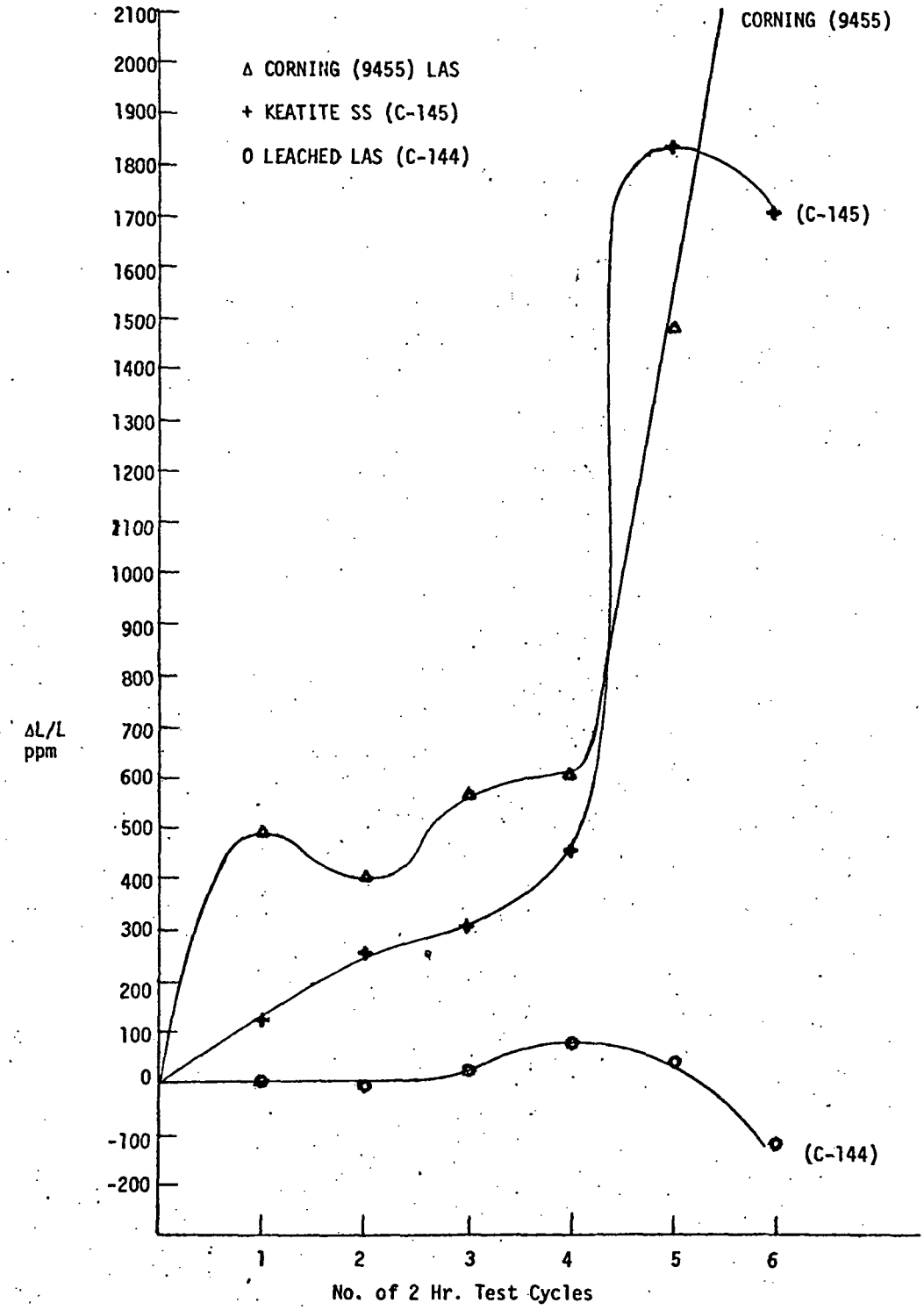

Figure 11 - Matrix Dimension Stability to 300°C Sulfuric Acid.
Method 1 - Acid Drained by Gravity with no Shaking.

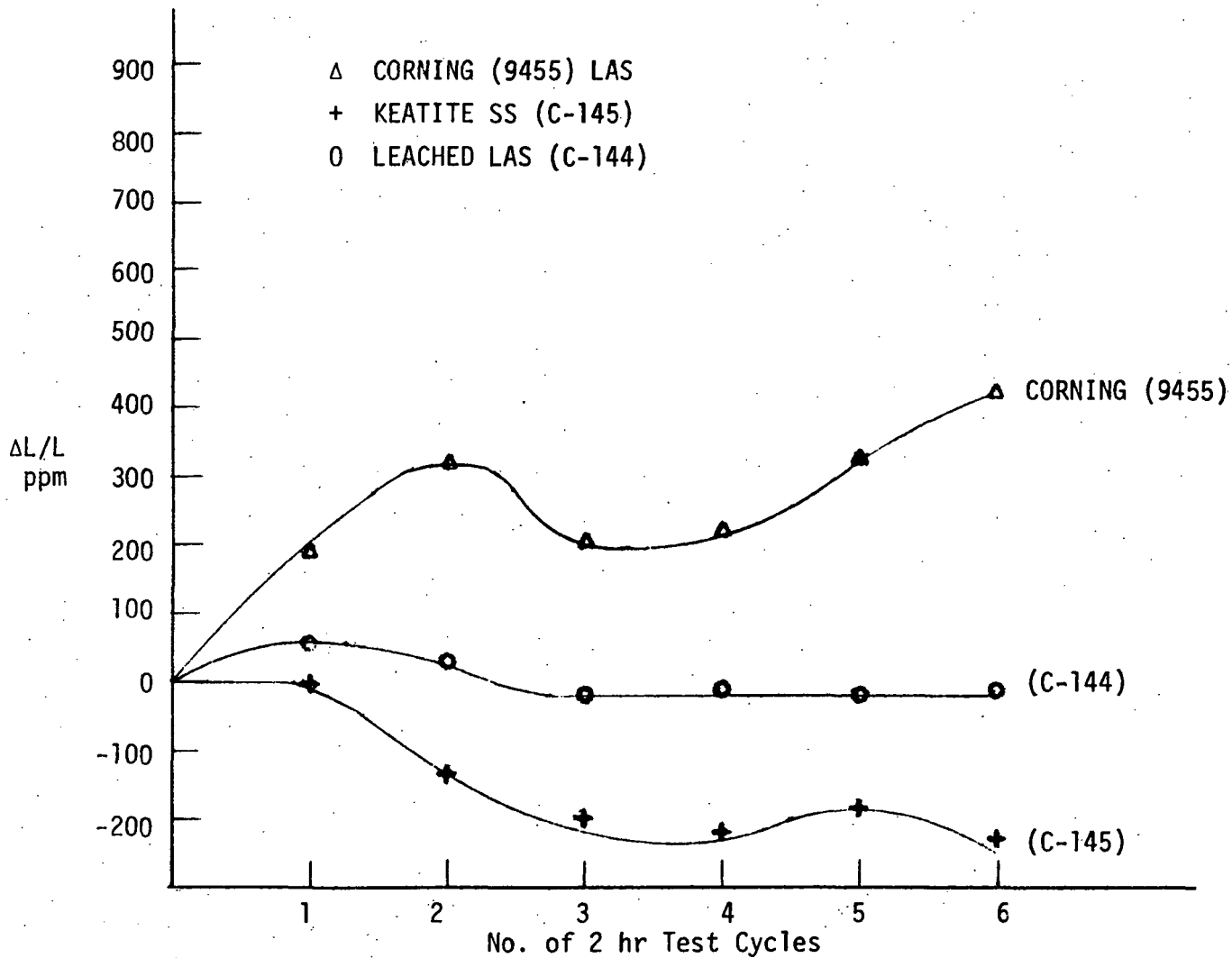

Figure 12 - Matrix Dimensional Stability to 300°C Sulfuric Acid. Method II - Acid Drained by Gravity and Shook Twice to Drain More Acid

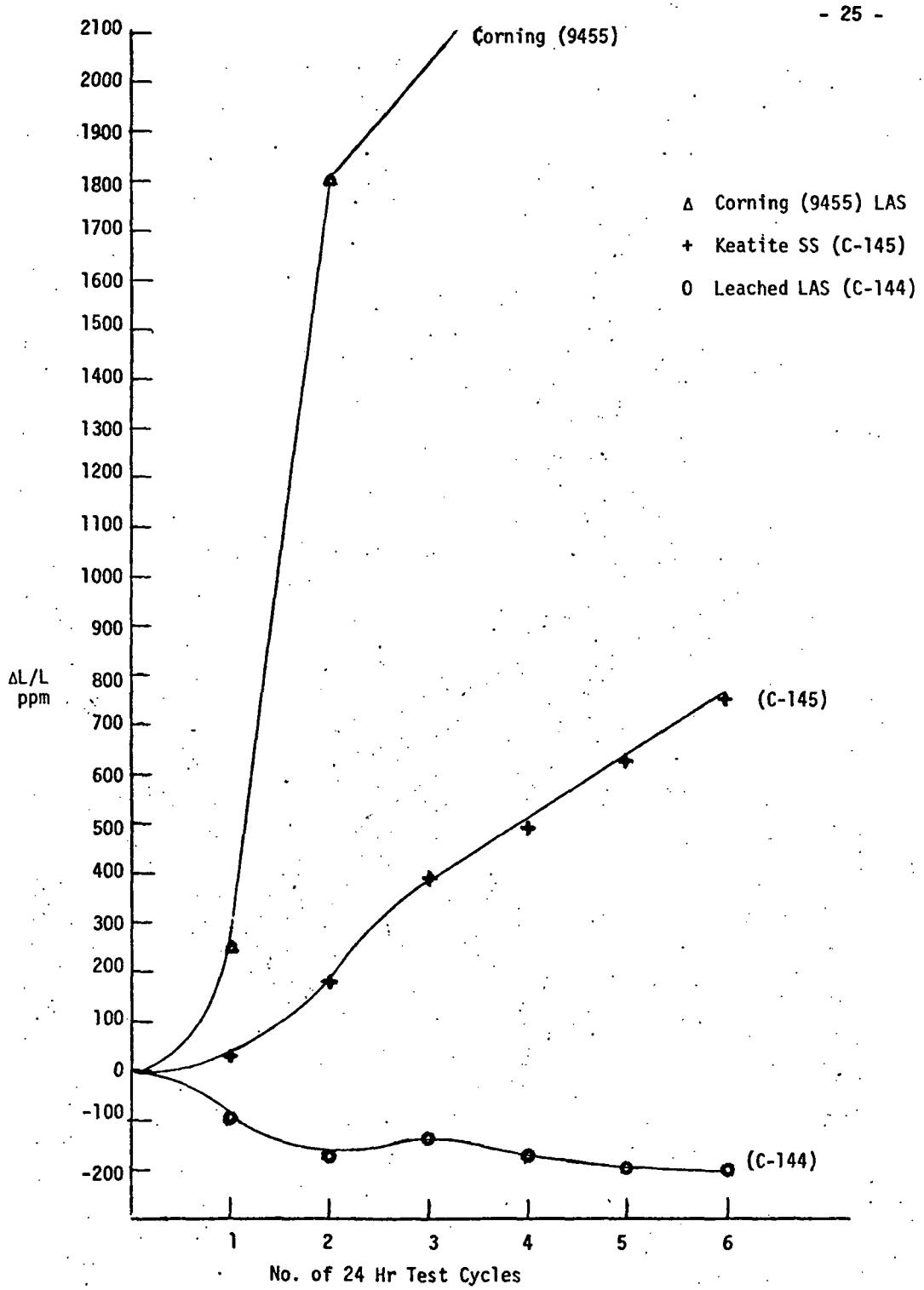

Figure 13 - Matrix Dimensional Stability to 1000°C Sodium Sulfate

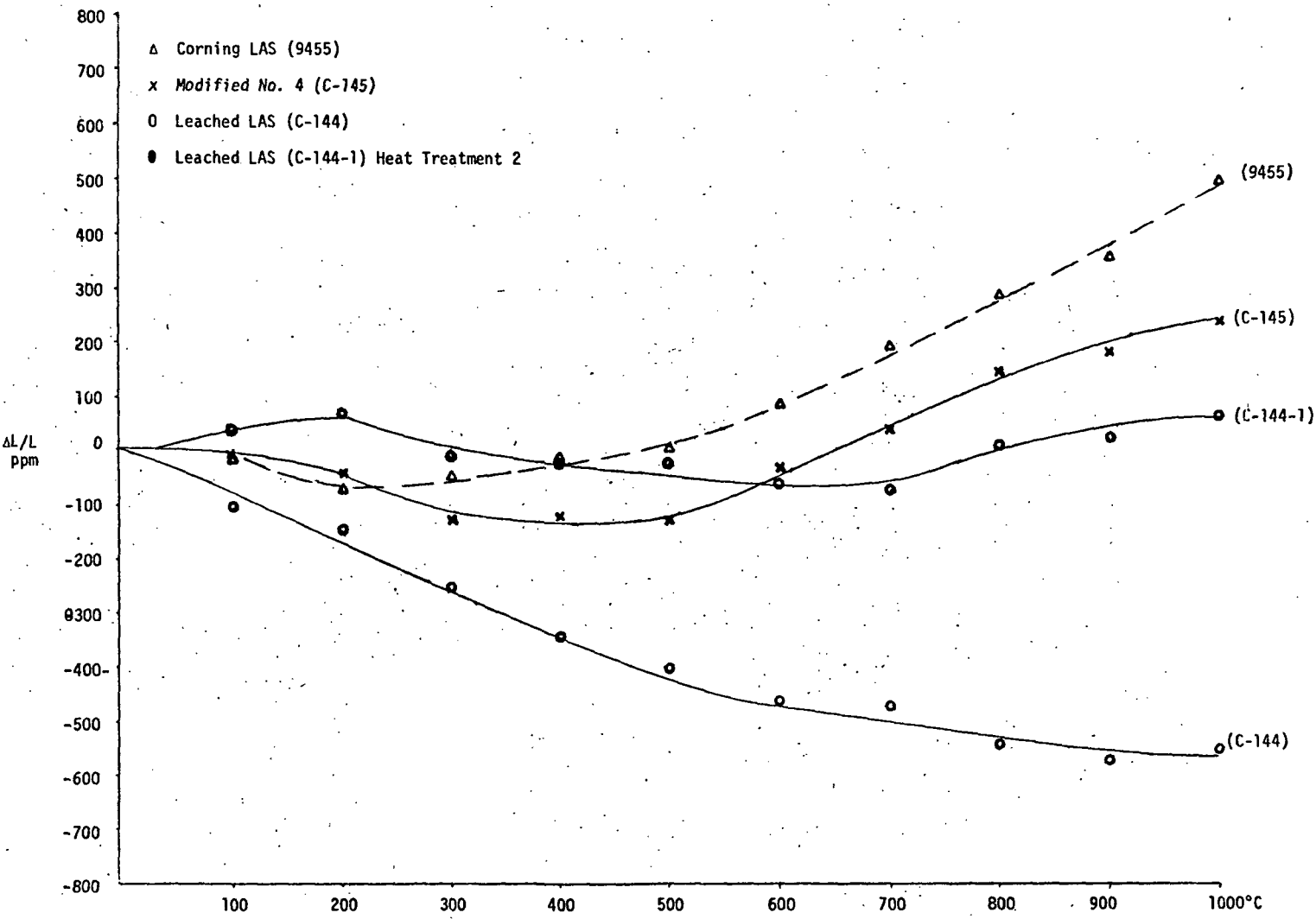

Figure 14 - Matrix Thermal Expansion of 9455 and C-144, C-144-1, C-145 after 1000°C-1 Hr

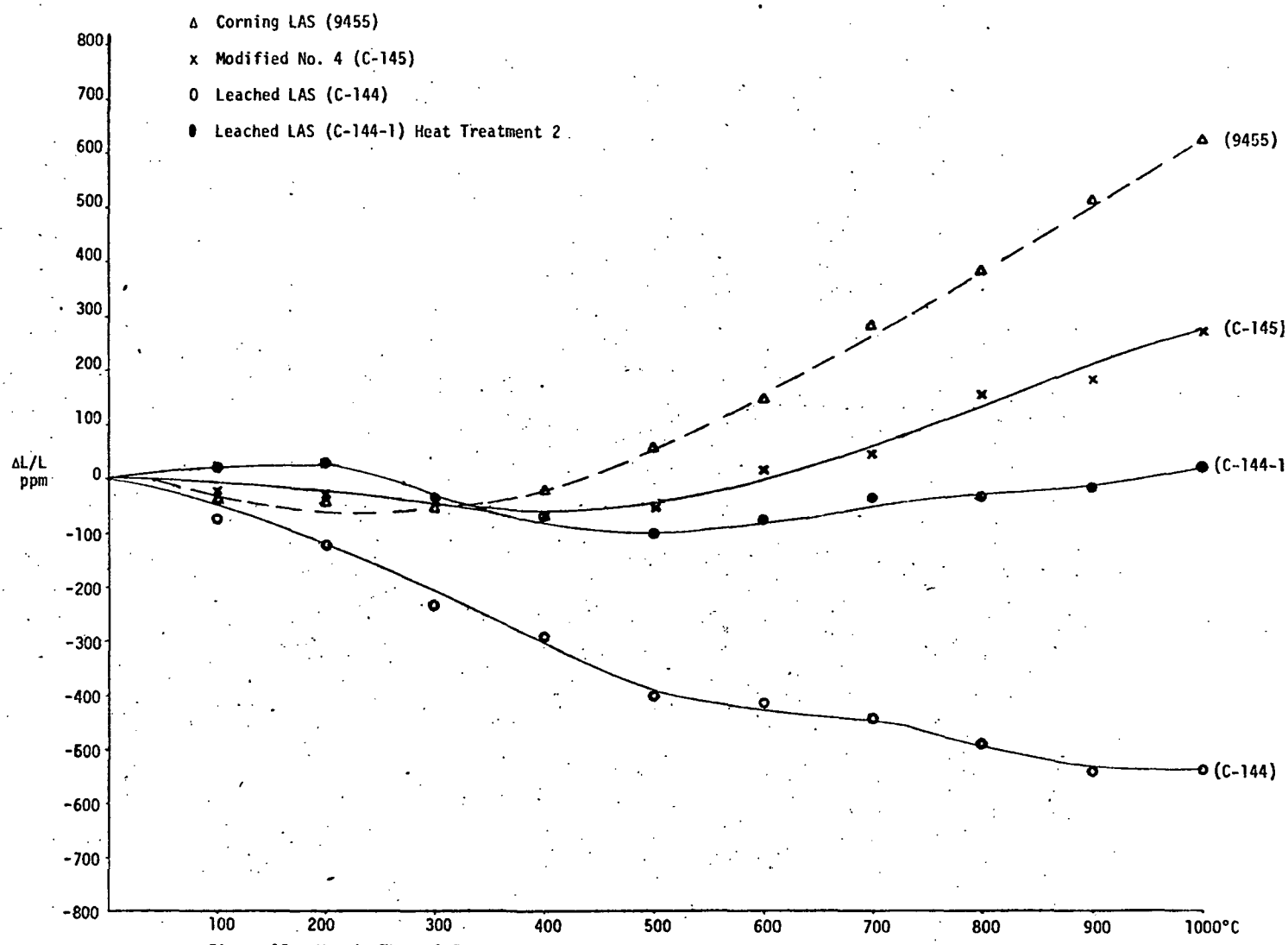

Figure 15 - Matrix Thermal Expansion of 9455 and C-144, C-144-1, C-145 after 1000°C-10 Hrs.

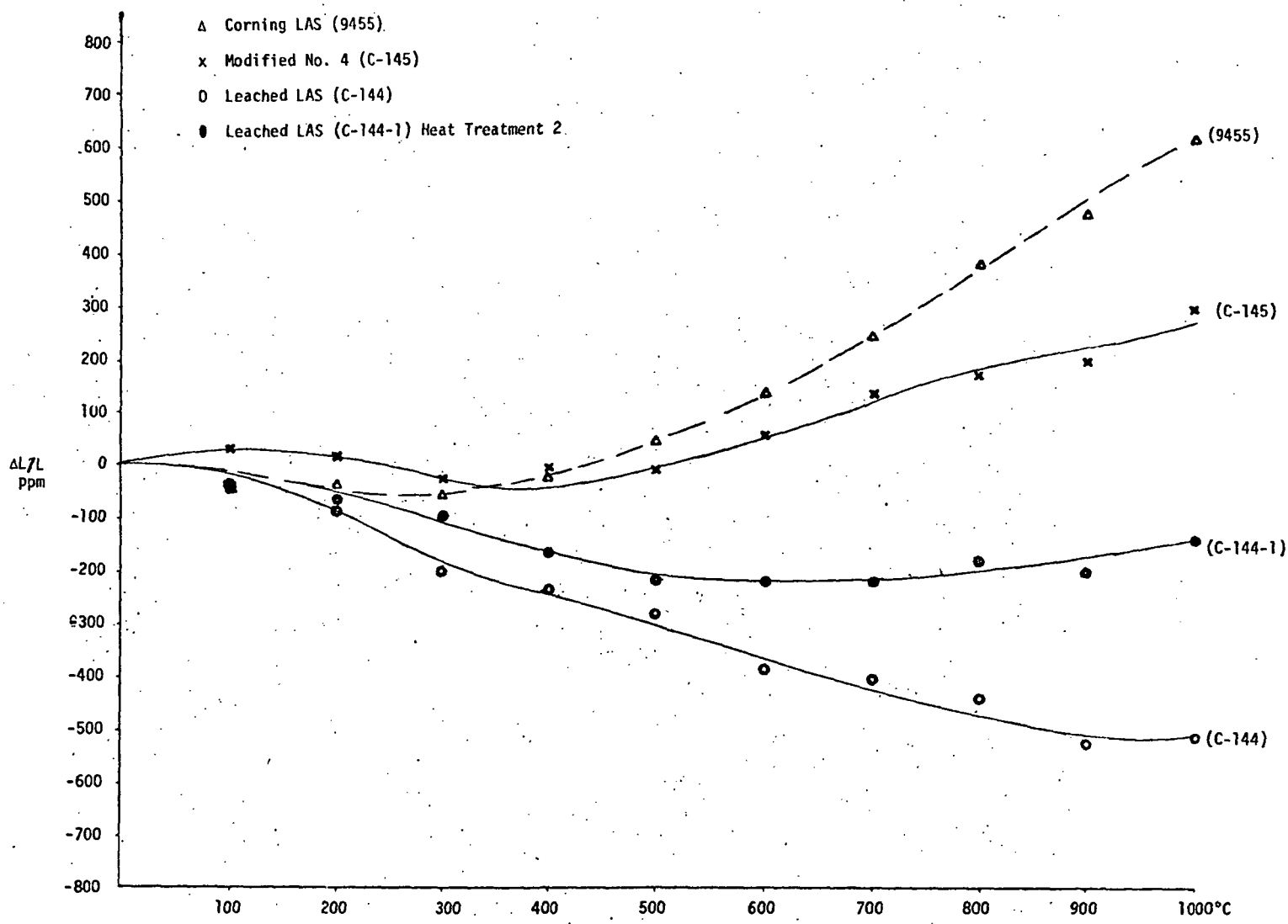

Figure 16 - Matrix Thermal Expansion of 9455 and C-144, C-144-1, C-145 after 1000°C-28 Hrs.

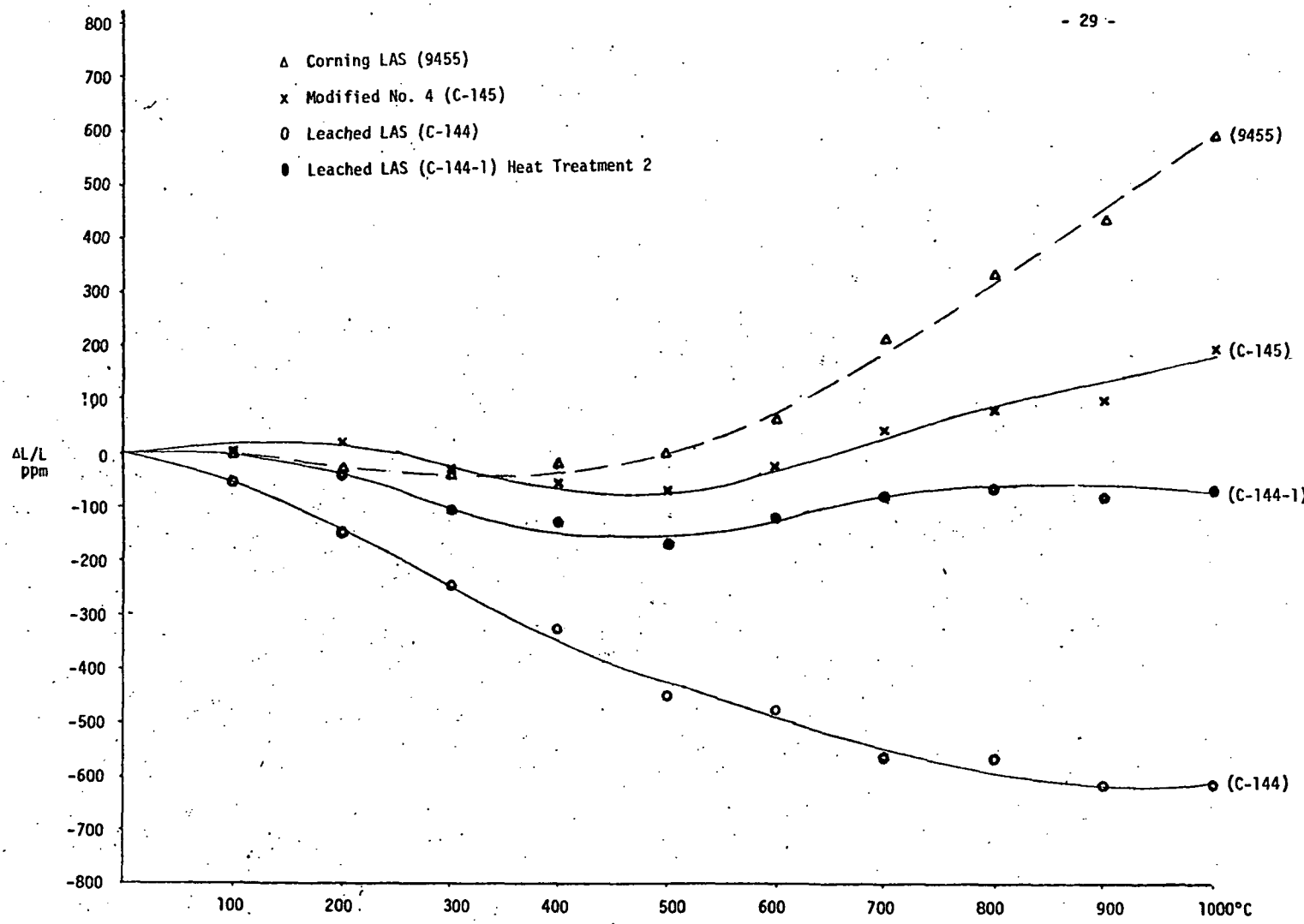

Figure 17 - Matrix Thermal Expansion of 9455 and C-144, C-144-1, C-145 after 1000°C-50 Hrs.

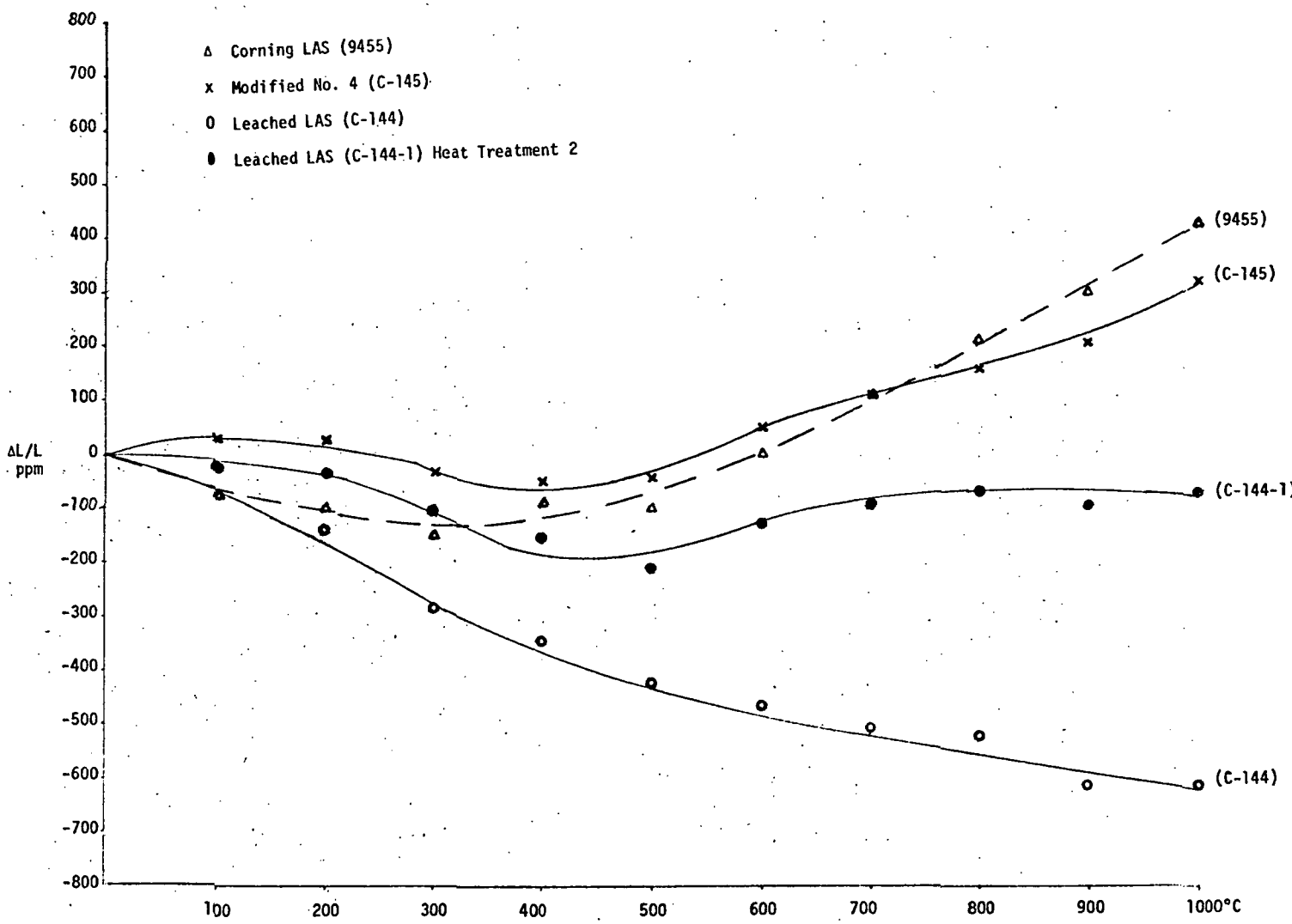

Figure 18 - Matrix Thermal Expansion of 9455 and C-144, C-144-1, C-145 after 1000°C-75 Hrs.

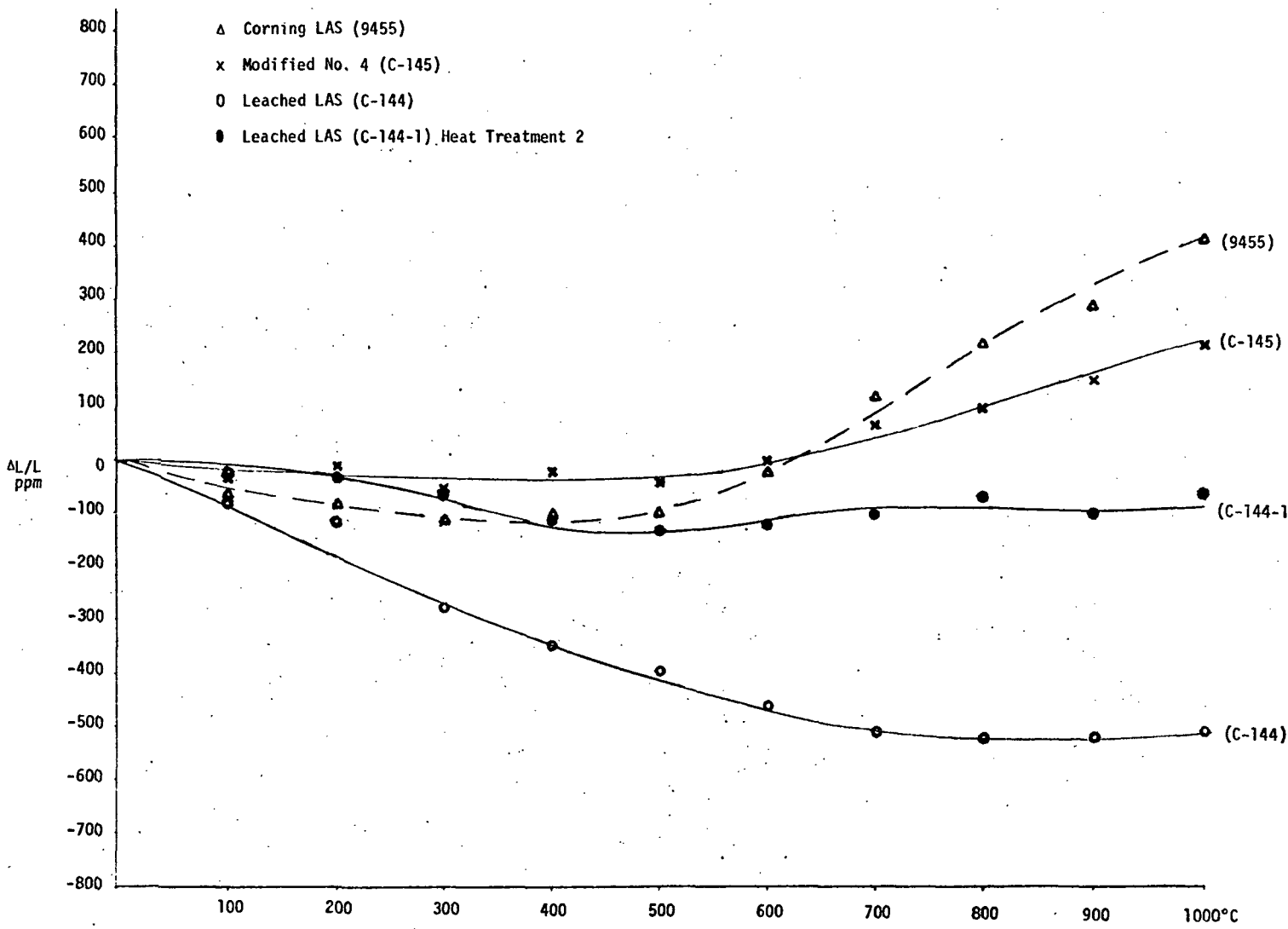

Figure 19 - Matrix Thermal Expansion of 9455 and C-144, C-144-1, C-145 after 1000°C-100 Hrs.

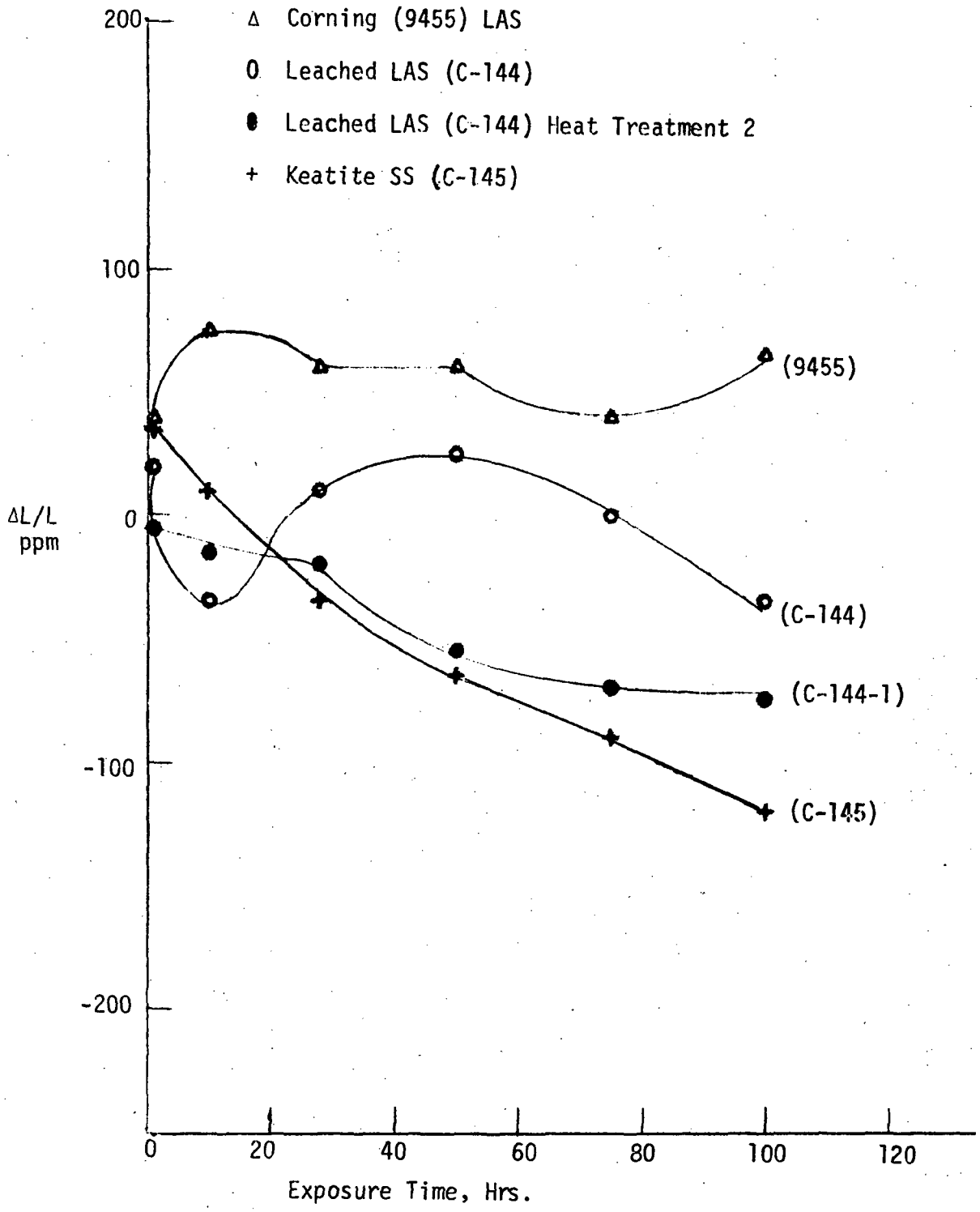

Figure 20 - Matrix Dimensional Stability at 1000°C, Length Change after Exposure.

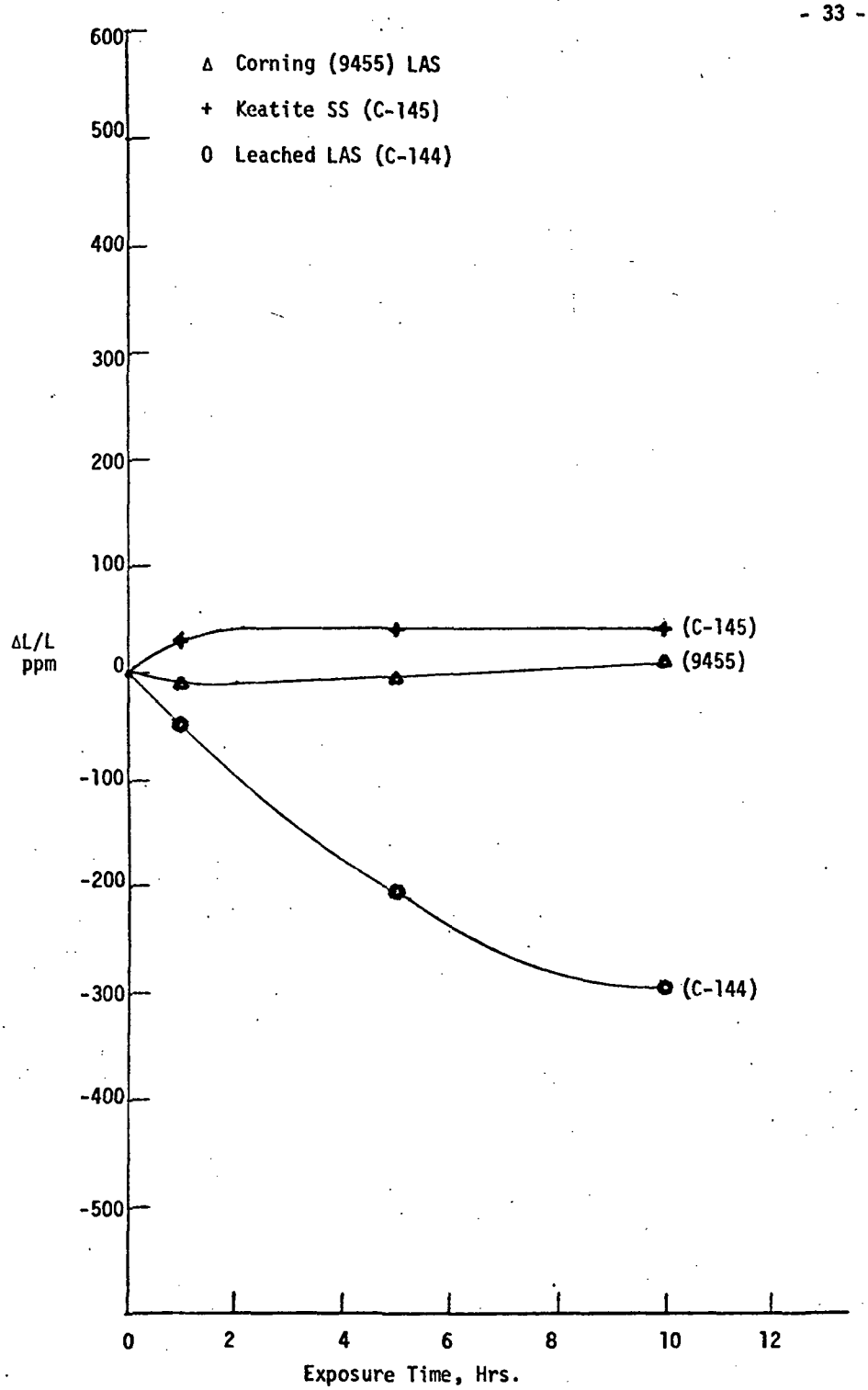

Figure 21 - Matrix Dimensional Stability at 1100°C, Length Change after Exposure.

FIGURE 13. GLASS-CERAMIC MATERIALS

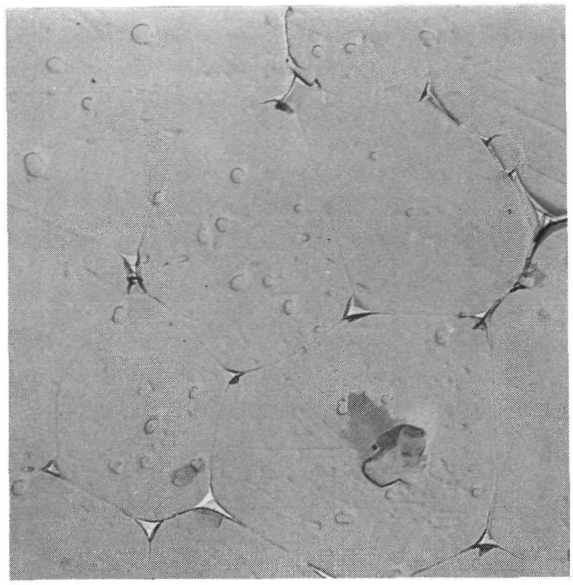

1 μ

MATERIAL 1

LMAS Quartz SS

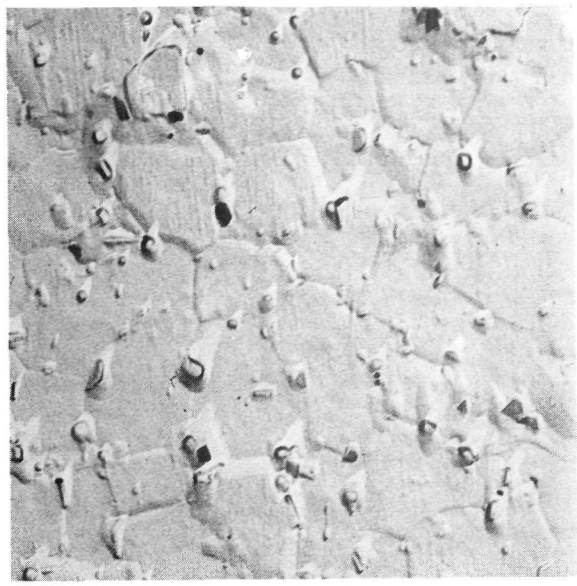

1 μ

MATERIAL 2

Keatite SS + Mullite

1 μ

C-144

Leached LAS

1 μ

C-145

Keatite SS